NAVAL POSTGRADUATE SCHOOL
Monterey, California

THESIS

HIGHLY PERVIOUS
LIQUID METAL TARGET SYSTEMS
FOR RADIOACTIVE ION BEAM GENERATION

by

Breckenridge S. Morgan

June 1999

Thesis Advisor: William B. Maier II
Second Reader: Robert F. Welton

Approved for public release; distribution is unlimited.

REPORT DOCUMENTATION PAGE

Form Approved OMB No. 0704-0188

1. AGENCY USE ONLY *(Leave blank)*	2. REPORT DATE	3. REPORT TYPE AND DATES COVERED
	June 1999	Master's Thesis

4. TITLE AND SUBTITLE
HIGHLY PERVIOUS LIQUID METAL TARGET SYSTEMS FOR RADIOACTIVE ION BEAM GENERATION

5. FUNDING NUMBERS

6. AUTHOR(S)
Morgan, Breckenridge S.

7. PERFORMING ORGANIZATION NAME(S) AND ADDRESS(ES)
Naval Postgraduate School
Monterey, CA 93943-5000

8. PERFORMING ORGANIZATION REPORT NUMBER

9. SPONSORING / MONITORING AGENCY NAME(S) AND ADDRESS(ES)
Oak Ridge National Laboratory
Oak Ridge, TN 37831

10. SPONSORING / MONITORING AGENCY REPORT NUMBER

11. SUPPLEMENTARY NOTES
The views expressed in this thesis are those of the author and do not reflect the official policy or position of the Department of Defense or the U.S. Government.

12a. DISTRIBUTION / AVAILABILITY STATEMENT
Approved for public release; distribution is unlimited.

12b. DISTRIBUTION CODE

13. ABSTRACT *(maximum 200 words)*

Radioactive ion beams (RIBs) of ^{69}As are currently needed for fundamental nuclear physics research and can be produced abundantly by proton bombardment of a liquid Ge target. In this thesis, we develop a series of highly pervious liquid target designs with mean diffusion paths several orders of magnitude less than traditional, pool-type, liquid targets. Experiments have been performed to identify materials (substrates) capable of suspending, through wetting, very thin layers of liquid Ge. Four candidate Ge-substrate target systems have been designed, and ^{69}As production may be significantly increased over previous targets. The target systems designed include liquid Ge coated onto an (i) inclined W plane, (ii) a long thin Mo wire birdsnest, (iii) a SiC weave and (iv) SiC coated C foam. A universal Ta target holder coupling the target to an ion source has also been designed and features a cooled re-circulating baffle for testing of each of the above target concepts. The results of long-term heating tests on the Mo wire birdsnest show its lifetime to be less than 100 hours; however, future online tests of short duration will test ^{69}As production for the birdsnested target. Ge did not wet the SiC weave target. The methods and design formulations developed in this thesis are applicable to a variety of RIB species produced from liquid targets.

14. SUBJECT TERMS
Radioactive Ion Beam, Isotope Separation Online, Germanium, Arsenic, Holifield Radioactive Ion Beam Facility, HRIBF, Oak Ridge National Laboratory, ORNL, Liquid Metal Targets

15. NUMBER OF PAGES
90

16. PRICE CODE

17. SECURITY CLASSIFICATION OF REPORT	18. SECURITY CLASSIFICATION OF THIS PAGE	19. SECURITY CLASSIFICATION OF ABSTRACT	20. LIMITATION OF ABSTRACT
Unclassified	Unclassified	Unclassified	UL

NSN 7540-01-280-5500

Standard Form 298 (Rev. 2-89)
Prescribed by ANSI Std. 239-18

Approved for public release; distribution is unlimited

HIGHLY PERVIOUS LIQUID METAL TARGET SYSTEMS FOR RADIOACTIVE ION BEAM GENERATION

Breckenridge S. Morgan
Lieutenant, United States Navy
B.S., The Citadel, 1991

Submitted in partial fulfillment of the
requirements for the degree of

MASTER OF SCIENCE IN APPLIED PHYSICS

from the

NAVAL POSTGRADUATE SCHOOL
June 1999

Author: _____
Breckenridge S. Morgan

Approved by: _____
William B. Maier II, Thesis Advisor

_____
Robert F. Welton, Second Reader

_____
William B. Maier II, Chairman
Department of Physics

ABSTRACT

Radioactive ion beams (RIBs) of ^{69}As are currently needed for fundamental nuclear physics research and can be produced abundantly by proton bombardment of a liquid Ge target. In this thesis, we develop a series of highly pervious liquid target designs with mean diffusion paths several orders of magnitude less than traditional, pool-type, liquid targets. Experiments have been performed to identify materials (substrates) capable of suspending, through wetting, very thin layers of liquid Ge. Four candidate Ge-substrate target systems have been designed, and ^{69}As production may be significantly increased over previous targets. The target systems designed include liquid Ge coated onto an (i) inclined W plane, (ii) a long thin Mo wire birdsnest, (iii) a SiC weave and (iv) SiC coated C foam. A universal Ta target holder coupling the target to an ion source has also been designed and features a cooled re-circulating baffle for testing of each of the above target concepts. The results of long-term heating tests on the Mo wire birdsnest show its lifetime to be less than 100 hours; however, future online tests of short duration will test ^{69}As production for the birdsnested target. Ge did not wet the SiC weave target. The methods and design formulations developed in this thesis are applicable to a variety of RIB species produced from liquid targets.

TABLE OF CONTENTS

LIST OF FIGURES

LIST OF TABLES

LIST OF SYMBOLS, ACRONYMS, AND/OR ABBREVIATIONS

a	Half the thickness of a foil used in estimating fractional yield of radioisotopes released from a surface.
α	Dimensionless Parameter for determining yield of desired species from a surface.
B	Measure of the penetration through the electron shells
D	Diffusion Coefficient
D_o	Diffusion Constant
D_m	Diffusion Coefficient at the melting point
dE/dx	Change in energy per unit length
E	Energy
E_1	Incident beam energy
E_2	Beam exit energy
F_r	Fraction of particles released.
H_D	Apparent Activation Energy of Diffusion
$I_s(1/\sqrt{\alpha})$	Modified Bessel function of the first kind of order s
I	Flux of projectile particles
K	Accelerating capability of a cyclotron
M	Atomic mass of the material in AMU
m	Mass of the ion in AMU
n	Number of atoms per cm^3
η	Packing density of atoms
q	Charge of ion
R	Gas Constant
R	Production Rate
φ	Effective Hard-Sphere diameter
σ	Nuclear Cross Section
T	Temperature of material in Kelvin
T_m	Temperature of the material at the melting point in Kelvin
$\tau_{½}(^{69}As)$	Half-life of ^{69}As (15.1 minutes)
τ_d	Measured delay time of a radioactive species from a specific material.
$\bar{\tau}$	Mean radioactive species lifetime
v	Velocity of electron
V	Atomic Volume
V_m	Atomic volume of the material at the melting point.
$\bar{x}$	Mean diffusion path length
Z	Atomic Number (Z protons)
Z_1	Atomic number of the incident beam

As	Arsenic (^{69}As – Enriched Isotope)
C	Carbon
Cu	Copper
Ge	Germanium (^{70}Ge – Enriched Isotope)
Mo	Molybdenum
Ni	Nickel
Pt	Platinum
Sn	Tin
SiC	Silicon Carbide
Ta	Tantalum
W	Tungsten
Ti	Titanium (^{54,60}Ti – Enriched Isotope)
Xe	Xenon
CVD	Chemical Vapor Deposit
HRIBF	Holifield Radioactive Ion Beam Facility
HSC	HSC Chemistry used in Outokumpu HAS Chemistry for Windows, Chemical Reaction and Equilibrium Software with extensive Thermochemical Database.
In situ	In Situation – the target is in place for proton bombardment.
ISOL	Isotope Separation Online
ORIC	Oak Ridge Isochronous Cyclotron
RADBEAM2	Computer Program using Monte Carlo techniques for calculating production rate of radioactive atoms from various nuclear reactions.
RIB	Radioactive Ion Beam
RVC	Reticulated Vitreous Carbon
SRIM	The Stopping and Range of Ions in Matter
Thickness	Density · length (Technical Term for RADBEAM2)
TIS	Target ion Source
TRIM	Transport of Ions in Matter
UNISOR	University Isotope Separation at Oak Ridge

ACKNOWLEDGMENT

The author would like to acknowledge the financial support of the Department of Energy through the Oak Ridge Associated University. This work was performed at the Holifield Radioactive Ion Beam Facility at Oak Ridge National Laboratory who provided equipment and additional support.

The author wants to thank first and foremost, Dr. Robert F. Welton for his guidance and patience during the work in performing this thesis.

Also, Syd Murray was irreplaceable in guiding me in the preparation of materials and the proper operation of the Bell Jar. Cecil Williams for his expertise in completing drawings and having the targets assembled. Dan Stracener for assistance during tests with the Ion source. Ken Carter for ensuring the funding and coordination efforts were complete. Jan Kormicki for his conducting the SIC wetting experiment in my absence. Mark Janney and Rick Lowden in the Metals and Ceramics Division at Oak Ridge National Laboratory for useful dialogue about the material properties of the samples evaluated.

Finally, I want to thank Dr. William B. Maier II for his guidance, efforts and, most importantly, patience during my education at the Naval Postgraduate School.

I. INTRODUCTION

A. PURPOSE

This thesis investigates designs of new-concept liquid metal targets for the production of radioactive ion beams (RIBs). A wide variety of radioactive species are best produced from targets which operate in the liquid state. Traditionally, these targets have been constrained in a contiguous, pool-style container. We explore the possibility of using an open, highly pervious liquid target configuration as an alternative to these traditional systems. We investigate the use of various materials to suspend liquids in thin layers in order to reduce the path length over which the radioactive particles must diffuse before leaving the liquid. Through judicious selection of substrate materials, thin layers of liquid target material can be held in place by a wetting process. Specifically, ^{69}As is currently produced at the Holifield Radioactive Ion Beam Facility (HRIBF) using a conventional pool-style target of liquid ^{70}Ge. We have investigated several highly pervious target configurations which optimize the production and release of ^{69}As from ^{70}Ge to provide increased beam intensities. Radioactive beams of ^{69}As are used in fundamental nuclear physics research conducted at the HRIBF.

B. RADIOACTIVE ION BEAM PRODUCTION

1. Concept of a RIB Facility

Beams of stable ions were first observed by Goldstein in 1886. Since then, the application of ion beams has grown steadily and now spans many fields of science and technology. The technology to produce ions has simultaneously grown to meet the challenges of the vast array of applications [1]. Recently, the demand for radioactive ion beams used in nuclear physics experiments has led to the development of specific technologies for RIB production. Both the demand

and supply of RIBs has, in turn, led to the planning and construction of several large scale facilities found worldwide [2,3]. The HRIBF located in the Oak Ridge National Laboratory, produces radioactive ions, by light ion bombardment of thick target materials by fusion-evaporation reaction and proton induced fission reactions of actinide targets. This technique, known as Isotope Separation On-Line (ISOL), is commonly used in many RIB facilities operating today. Alternatively, RIBs can be produced by passing heavy ions through a collision gas and collecting the forward scattered nuclear reaction products and forming them into a beam. This technique is known as projectile fragmentation and is best suited for RIBs of very short half-lives [4].

Ultimately RIBs delivered to experiments at various energies are used in fundamental nuclear research. The measurement of cross sections of nuclear reactions involving RIBs are important in understanding the structure of the nucleus, i.e. verification of the standard model. In addition, thin targets are employed at experimental stations to produce very short lived radioactive species very far from the valley of nuclear stability [5] which can be resolved by various recoil type spectrometers and sensitive gamma ray detectors [6].

2. ISOL Technique

The ISOL technique was developed in Europe approximately 30 years ago and used to produce low energy (keV) RIBs. In this technique a low energy, high current driver accelerator bombards thick refractory target material maintained at high temperatures with a light ion beam. Radioactive nuclei produced within the target material are released and transported to a nearby ion source. The extracted radioactive beam is then accelerated by a post-accelerator (typically a high energy, low current machine). A schematic representation of this process is illustrated in Figure 1, and Table 1 lists the major facilities which produce RIBs using the ISOL technique [2].

Facility	Location	Driver Accelerator	Driver Beam Energy	Post Accelerator	RIB Energy (MeV/AMU)	Status
ARENAS	Louvain La Neuve, Belgium	Cyclotron	80 MeV	LINAC	1.5	Operational
HRIBF	Oak Ridge, Tennessee, USA	Cyclotron	55-86 MeV	Tandem	5	Operational
SPIRAL at GANIL	Caen, France	Cyclotron	100 MeV	LINAC	5-50	Project
ISAC at TRIUMF	Vancouver, Canada	Cyclotron	440 MeV	LINAC	1.5	Operational
REX-ISOLDE	Geneva, Switzerland	Synchrotron	1 GeV	LINAC	1	Operational
Moscow	Moscow, Russia	LINAC	600 MeV	LINAC	6.5	Project

Table 1. Various Radioactive Ion Beam (ISOL) Facilities Worldwide after Ref. [2]

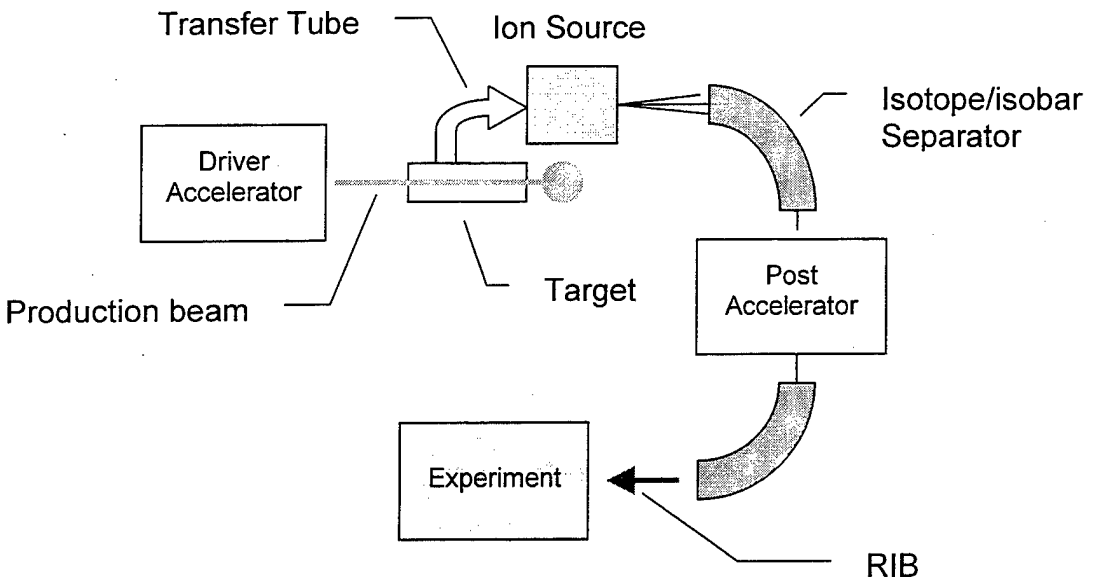

Figure 1. Overview of the ISOL Process

At the HRIBF, the Oak Ridge Isochronous Cyclotron (ORIC) serves as the driver accelerator for the facility. ORIC is designed as a K = 105 cyclotron where the quantity K describes the accelerating capability of a cyclotron and is expressed as

$$K = \frac{m \cdot E}{q^2}. \qquad (1.1)$$

Here, the quantities m and q are the mass and charge of the ions composing the driver beam in atomic units and E is the beam energy in MeV. However, practical limitations involving ion beam extraction limit the intensities of protons to approximately 50 μA at 50 MeV [7]. The driver beam is then directed onto thick target material contained within a dedicated target/ion source (TIS). Radioactive atoms are ionized in the TIS and accelerated nominally to 40 kV on an isolated high voltage platform. These ions undergo first stage mass analysis by a split pole, low resolution, mass analyzing magnet ($\Delta m/m \sim 1000$) located on the high voltage platform.

Electrostatic beam focusing elements direct the beam through an ~ 260 kV graded accelerator column. The 300 kV beam now undergoes high resolution mass/isobar separation ($\Delta m/m$ ~ 10,000 – 20,000) prior to injection into the tandem accelerator. The electrostatic tandem accelerator serves as the post accelerator for this facility and can operate with a terminal voltage as high as 25 MV. Typically, this accelerator can accelerate species as heavy as 90 AMU to energies of several MeV per nucleon [7]. The RIB is then delivered to one of several large-scale experimental facilities located at the HRIBF. These facilities include a recoil mass spectrometer for nuclear structure experiments, the Daresbury Recoil Separator for astrophysics experiments and the Enge Mass Spectrometer for nuclear reaction studies [6].

3. RIB Target/Ion Source

In general, each new RIB species requires significant development effort since nuclear reaction products are produced in limited quantities and undergo substantial losses prior to ionization due to radioactive decay and physical and chemical interactions with the target/ion source [8]. Often, whether or not a RIB can even be produced at all depends on how well the TIS has been designed for a given species. Each radioactive atom entering the RIB must first diffuse through the target material, desorb from its surface, be transported to the ion source, and finally, undergo ionization. All of these steps must occur before the radioactive atom decays into daughter species and lost. If the target material has a high density with characteristic dimensions on the order of mm then diffusion is usually the dominant loss process.

An example of a design of a RIB TIS is shown in Figure 2. Beam enters the target material shown, on an axis perpendicular to the plane of the paper. Depending on the atoms required for the desired nuclear reaction, this target material can be in either in the solid or liquid state. The target container is heated radiatively by a single pass Ta heater which is heated by directly flowing

several hundred amperes of DC current through it. Target temperature is maintained at the highest temperature that the target material can withstand to ensure maximum diffusion rates and volatility of radioactive species. Radioactive atoms (vapors) enter a horizontal Ta vapor transport tube, shown in the figure, which is maintained at temperatures of ~ 1800°C to prevent condensation of these atoms on the surface. Upon arrival at the ionization region, some form of ionization followed by ion beam extraction takes place. In the case of the ion source shown in the figure, electron impact ionization ensues as a result of electrons accelerated into the ionization region from a 2100°C emission surface [9]. A conical extraction electrode accelerates the newly formed radioactive ions into a beam for injection into the post accelerator.

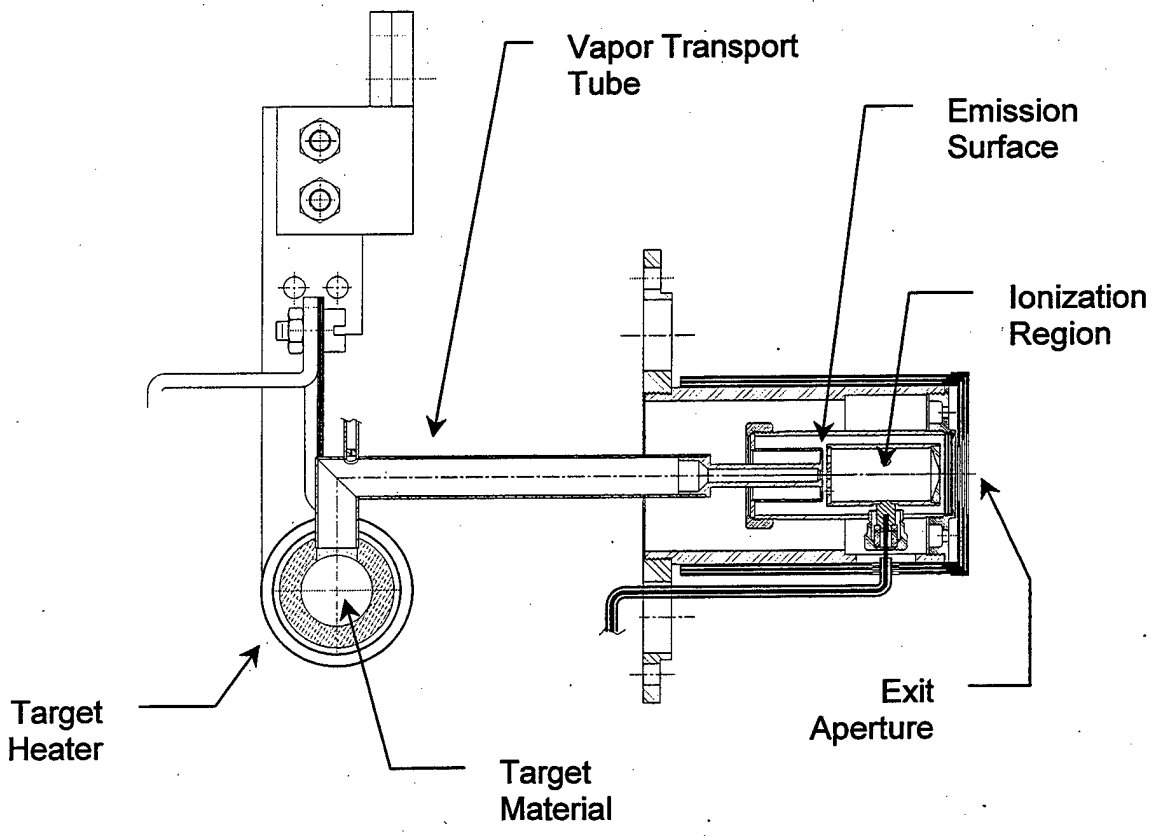

Figure 2. General Overview of the Target Ion Source

C. BACKGROUND OF LIQUID METAL TARGETS

1. Traditional ISOLDE Liquid Targets

Traditional liquid targets used in RIB generation had been initially developed at ISOLDE which is located in the CERN accelerator facility. These targets are based on a cylindrical container which holds the liquid in a pool-type configuration. Since liquid materials are in general less refractory (more volatile) than solid materials a cooled vapor baffle is usually employed to prevent the entrance of target material vapor into the ion source [10]. ISOLDE is a radioactive ion beam facility which has produced low energy RIBs for many years and has developed much of the TIS technology [3]. The driver accelerator at ISOLDE can produce 1 – 2 μA of 1 GeV protons.

2. New ISOLDE Targets: Pt and Sn in Carbon powder

The ISOLDE group has found that if fine droplets of liquid material which do not react with graphite are suspended in a fine mesh of graphite powder, the release of short lived radioactive species can be enhanced. Specifically, targets of Pt or Sn were developed [11]. This has the effect of reducing the length a radioactive atom must travel within the target material before it can be released from the surface. The authors point out that this technique is limited to materials, which do not form carbides with the graphite powder. This greatly narrows the scope of the technique to target materials which exhibit no chemistry with C.

3. First Generation HRIBF Liquid Targets

Liquid metal targets used at the HRIBF have so far been limited to Ge for the production of radioactive As. A pool of the target material was held in a contiguous volume within a cylindrical graphite container. During operation, this target material attained temperatures 1560°C which was required to achieve efficient release of the radioactive As from this thick target material. Radioactive atoms were released from a Ge surface with dimensions of 4.2 x 9.6 mm resulting in a surface area of 40 mm^2. This configuration is shown in Figure 3.

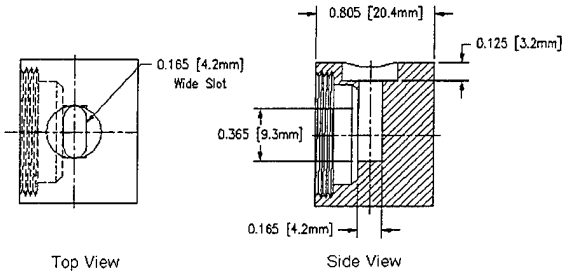

Figure 3. First Generation Liquid Ge HRIBF Target Configuration

D. MOTIVATION

One RIB experiment of current interest explores the various models of sub-barrier fusion and the role of the proton transfer in the $^{69}As + ^{46,50}Ti$ reaction [12]. The current HRIBF liquid Ge target has been operated up to temperatures as high as 1560°C with a maximum yield of $2x10^6$ ^{69}As ions per second observed [7]. The sub-barrier fusion experiment requires RIBs of ^{69}As on the order of 10^7 particles per second. Thus, a liquid Ge target with yields exceeding 10^7 particles per second is necessary for the successful completion of this experiment.

The principle drawback of the first-generation HRIBF target seems to be decay losses incurred before release of As from the target material. Release

times measured from this target system for As in Ge have been observed to be 3.6 hours. Release time is defined as the average length of time after creation a radioactive particle remains in the TIS [13]. After the experiment, the TIS was rapidly cooled and an autopsy performed in which each component of the TIS was isolated and counted with a gamma ray spectrometer. It was discovered that most of the As activity was still present in the target material. Thus, only a small fraction of the ^{69}As produced was released. Under steady state flow conditions, Equation 1.2 expresses the fraction F_r of an activity with a half-life of $\tau_{1/2}$ released after a period of being stored in a reservoir for τ_d seconds [14].

$$F_r = \frac{\tau_{1/2}}{\tau_{1/2} + \tau_d} \tag{1.2}$$

For the case of ^{69}As ($\tau_{1/2}$ = 15.1 minutes) in ^{70}Ge (τ_d = 3.6 hours), equation 1.2 shows that the fractional release is on the order of 0.065. Considering the results of the autopsy, this means that only 6.5% of the ^{69}As produced was actually released from the target material.

In order to improve the release efficiency of ^{69}As from the target, we have sought to locate materials which are available in a highly pervious format that can serve to suspend the liquid target material by virtue of wetting phenomena exhibited between molten Ge and a substrate. We hope to reduce the path length that As must travel within the target material before arriving at the surface. The substrate material must be not decompose at high temperatures and should be readily wet by Ge. This thesis will develop a series of target systems which are characterized by decreased diffusion paths and hopefully faster release as compared with the first-generation targets.

Four target designs will be developed and examined; planar, birdsnested wire, foam, and fibrous target substrates are investigated here. All should be capable of operating at high temperatures. Selection of several candidate materials that will serve as the substrate to hold the liquid Ge will be the first

step. After selecting the materials which best suit each scheme, a computational analysis of the geometrical design of a target system will be performed to tailor each target to the driver beam energy. There is no strong previous evidence that points directly to the best material for the substrate. Some information exists which suggests viable crucible materials and indicates possible materials wet by Ge. None have been uncovered that provide the in-depth examination needed to make a well-informed decision. We have performed experiments to provide that information.

This technique of suspending very thin layers of liquid target material on a substrate is not limited to the case of ^{69}As produced from liquid ^{70}Ge. This method could find even greater applicability producing RIBs of very short-lived species which have hitherto now been completely inaccessible using conventional pool-type liquid targets. Equation 1.2 shows that to achieve a high fractional release of very short lived species, τ_d must be small compared with $\tau_{1/2}$. Therefore, we suspect this technique should be particularly applicable to very short-lived species such as ^{58}Cu ($\tau_{1/2}$ = 3.2 s) produced from a liquid ^{58}Ni target provided a suitable substrate could be found for liquid Ni.

II. EVALUATION OF CANDIDATE SUBSTRATE MATERIALS

A substrate material would need to be refractory, wetable, structurally sound, and have a low Z. The substrate must also have a low vapor pressure. For the various target designs that will be considered by this thesis, Ge surface tension must be overcome by adhesion between substrate and liquid Ge so that the Ge will spread out and cover the substrate. The thin layer of Ge so formed will vastly increase surface production area. Ion sources are often in continuous operation for weeks at a time, so the substrate must maintain its integrity for long periods at high temperatures. In addition, the candidate substrate material should be as low Z as possible to minimize beam energy loss in the substrate. Finally, cost and availability are considered.

The candidate materials that were chosen with the above criteria are as follows: Tungsten (W), Molybdenum (Mo), Tantalum (Ta), Silicon Carbide (SiC). In addition to having a substrate, it is also necessary to have a crucible material. Graphite worked well as crucible material in first generation targets and was used in the wetting experiment as a target holder. An ideal target container should not be wet by the target material to force the liquid target onto the substrate. SiC was included because SiC is reported to be readily wet by Germanium and have low Z [15, 16].

A. EXPERIMENTAL EQUIPMENT

The Bell Jar is a high vacuum (10^{-6} - 10^{-7} Torr) system in which samples can be hated to temperatures in excess of 1100°C [17]. Tungsten strip heaters (ohmically heating) in either configuration one or two, as seen in Figure 4, reach temperatures of 1200°C – 1500°C. The temperature inside the test crucible ranges from 1050°C to 1350°C. When the non-melted material is placed inside

the test crucible, it is at a level approximately half the height of the container. A photograph of the bell jar apparatus can be found in Figure 5.

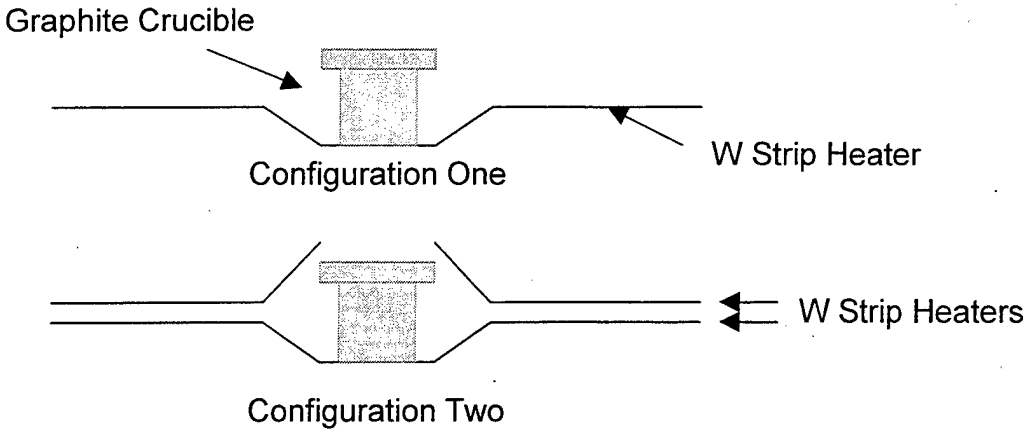

Figure 4. Crucible and Heater Configuration During Bell Jar Wetting Experiments.

A single-color optical pyrometer with an operating range of 700°C to 2200°C was used to take readings from either the strip heater or the crucible [18]. All weights were measured with a balance type scale sensitive to 0.0001 grams.

B. EXPERIMENTAL PROCEDURE

Once the dimensions of the candidate substrate and the appropriate amount of ^{70}Ge was determined, the ^{70}Ge was weighed and the substrate material was cleaned. The substrate was degreased, then cleaned with acetone, followed by ethyl alcohol and finally placed in an ethyl alcohol solution in an ultrasonic cleaner for at least 10 minutes. Prior to placing into the test crucible, the material was again rinsed with ethyl alcohol and blown dry.

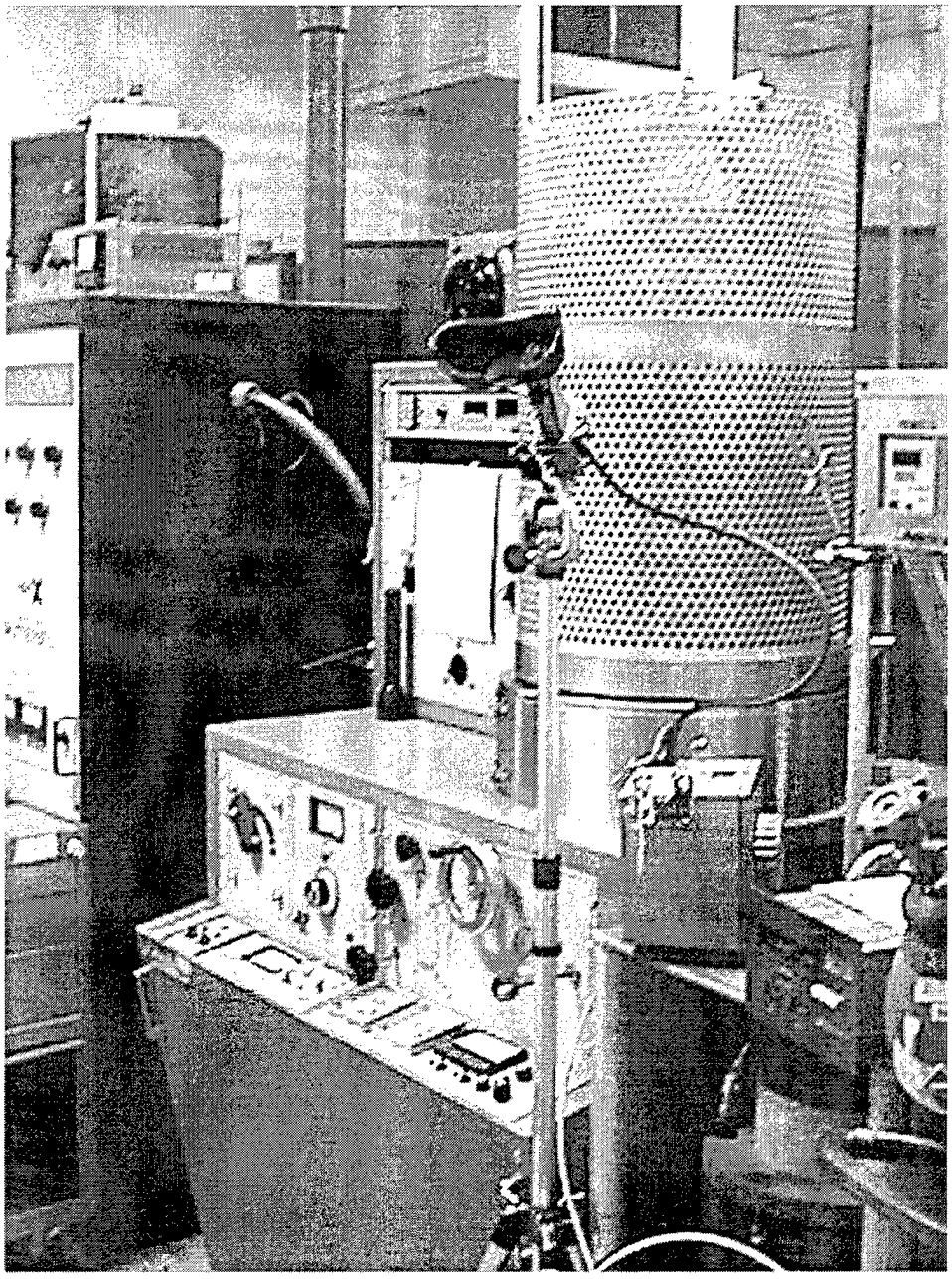

Figure 5. High Vacuum Bell Jar System

Depending on which experiment was being performed, the test crucible would either be in configuration one or two. In Configuration two, the upper tungsten strip had an opening that allowed direct observation of the material or was covered to reduce material evaporation. Once the material was in place in the test crucible, the system was evacuated and the test crucible was heated.

C. WETTING DATA

The following discussion is based on the data summarized in Tables 2 and 3. The experiments began on 5 November 1998 and were completed 14 December 1998. The SiC experiments were conducted in February and March of 1999. For the initial experiments, candidate materials were tested for their wetting properties. After the first round of tests, further experiments on varying configurations of candidate materials verified the results previously obtained and tested wetting properties in a configuration close to that which would be used as a RIB target. Figure 6 shows a Ge 250-μm coating on Mo wire. Figures 7 and 8 are the SiC fiber bundle prior to and after the wetting experiment. Figures 9 and 10 are the SiC fiber bundle ends prior to and after the wetting experiment.

D. MATERIAL SELECTION FOR CANDIDATE TARGETS

A suitable target requires material that Ge wets and that retains its structural integrity up to temperatures required for release of ^{69}As which can be as high as 1600°C. The experiments previously mentioned on tungsten, molybdenum, graphite, tantalum and SiC were conducted to determine the wetting characteristics of each material. During the experimentation phase, several prototype targets were considered and will be discussed in detail in the following chapter. These four designs are the Planar, Birdsnested, Fibrous, and Foam Targets. Target types were studied to evaluate the surface area available for release of ^{69}As.

#	Material	Form	Size	Comments	S/U/I
1	C*	Crucible	-	Material did not completely undergo phase change. No results.	I
2	Ta	Crucible	-	Ge was ejected from the crucible prior to successful completion. No results.	I
3	Mo	Crucible	-	Ge did wet and wick on Mo Crucible.	S
4	C*	Crucible	-	Ge did not wet or wick on the C*.	S
5	Ta	Crucible	-	No results.	I
6	W	Foil	9.3 mm	Ge appeared to wet the W foil	I
7	Ta	Crucible	-	Inconclusive, Vacuum was at 2×10^{-2} Torr at the end of the experiment.	U
8	Ta	Crucible	-	Ge did wet and wick on Ta Crucible.	S
9	Mo	Wire	*250 μm*	Ge wicked onto Mo wire and did not react with C* crucible.	S
10	Mo	Mesh	*30.48 μm*	Mo mesh and Ge were formed into a ball. The mesh appears to have collapsed, possibly due to the surface tension of the Ge.	U
11	W	Wire	*76.2 μm*	Ge did not wet or wick on the W wire. Ge did concentrate in the center of the W wire that had been birdsnested in the crucible.	S
12	Mo	Wire	*101.6 μm*	Ge wet and wicked up Mo wire.	S
13	Mo	Mesh Support Spring	*30.48 μm*	A W wire coil wound like a spring supported Mo mesh. Ge wet Mo mesh, but mesh was collapsed on one side of crucible. This collapse possibly occurred during cooling of material and not during actual liquid state of Ge. Additional test required where Mo mesh can be observed directly.	U
14	W	Wire	*76.2 μm*	Ge did not wet or wick on W wire. Ge did concentrate in center of the W wire that had been birdsnested in crucible.	S
15	Ta	Wire	*50.4 μm*	During heating process, after Ge had phase changed, the Ta mesh collapsed.	U

Table 2. Results of Ge wetting experiments 1 – 15 conducted at the HRIBF.

#	Material	Form	Size	Comments	S/U/I
16	Mo	Wire Support Spring	*30.48 μm*	W wire coil wound like a spring to support Mo mesh. Ge did not wet W as before and gathered in center of mesh.	S
17	Mo	Wire Extended Heating	*101.6 μm*	Mo wire was placed in C* crucible for 7 hours to determine the long terms affects of Ge on Mo. This wire held up much better than the 1.3 mil, but had indications of loss of structural integrity.	S
18	Mo	Wire Extended Heating	*250 μm*	Mo wire was placed in C* crucible for 5 hours to determine the long terms affects of Ge on a larger diameter Mo wire.	S
19	SiC	Fibers	*15 μm*	Ge appeared to wet SiC fibers. After SEM, appears Ge penetration and smooth coating in areas. Other areas had spheres of Ge which seem to be 50 – 500 *μm* in diameter. Online Testing later showed that SiC Fibers are not wet by Ge.	S
20	SiC	Foam	*100 μm*	Ge seems to wet SiC foam. 475 cm^2/g surface area.	S

C* = Graphite

Table 3. Results of Ge wetting experiments 16 – 20 conducted at the HRIBF

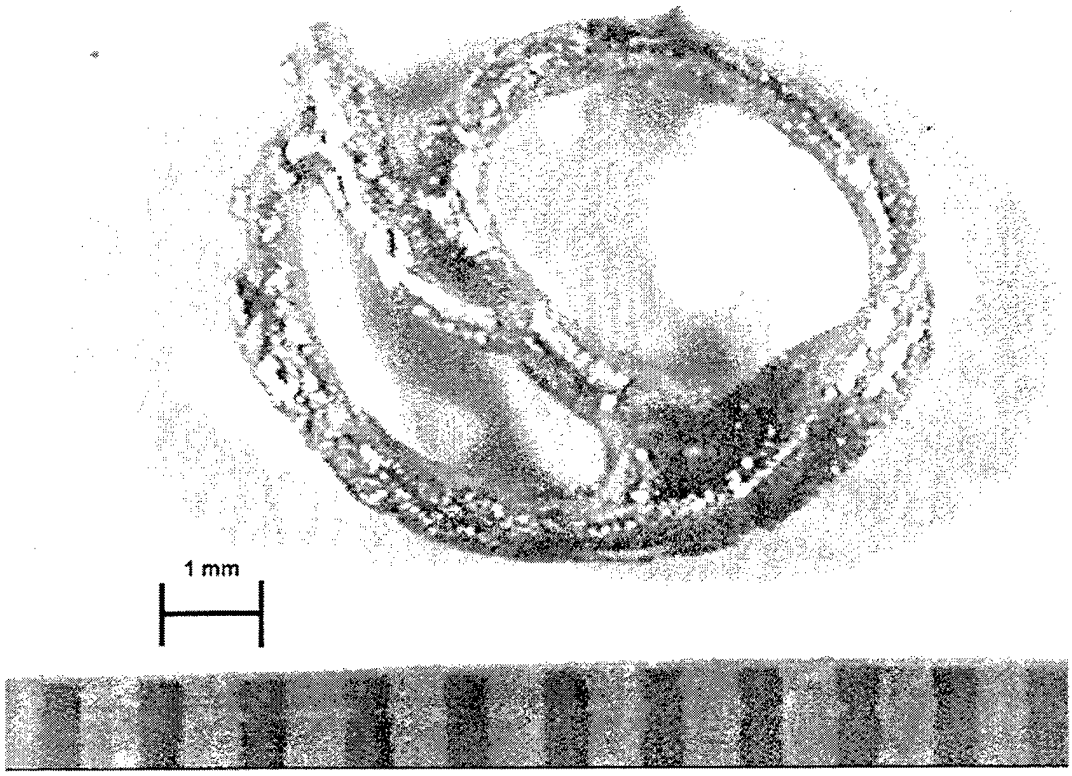

Figure 6. Ge Wet onto Mo Wire

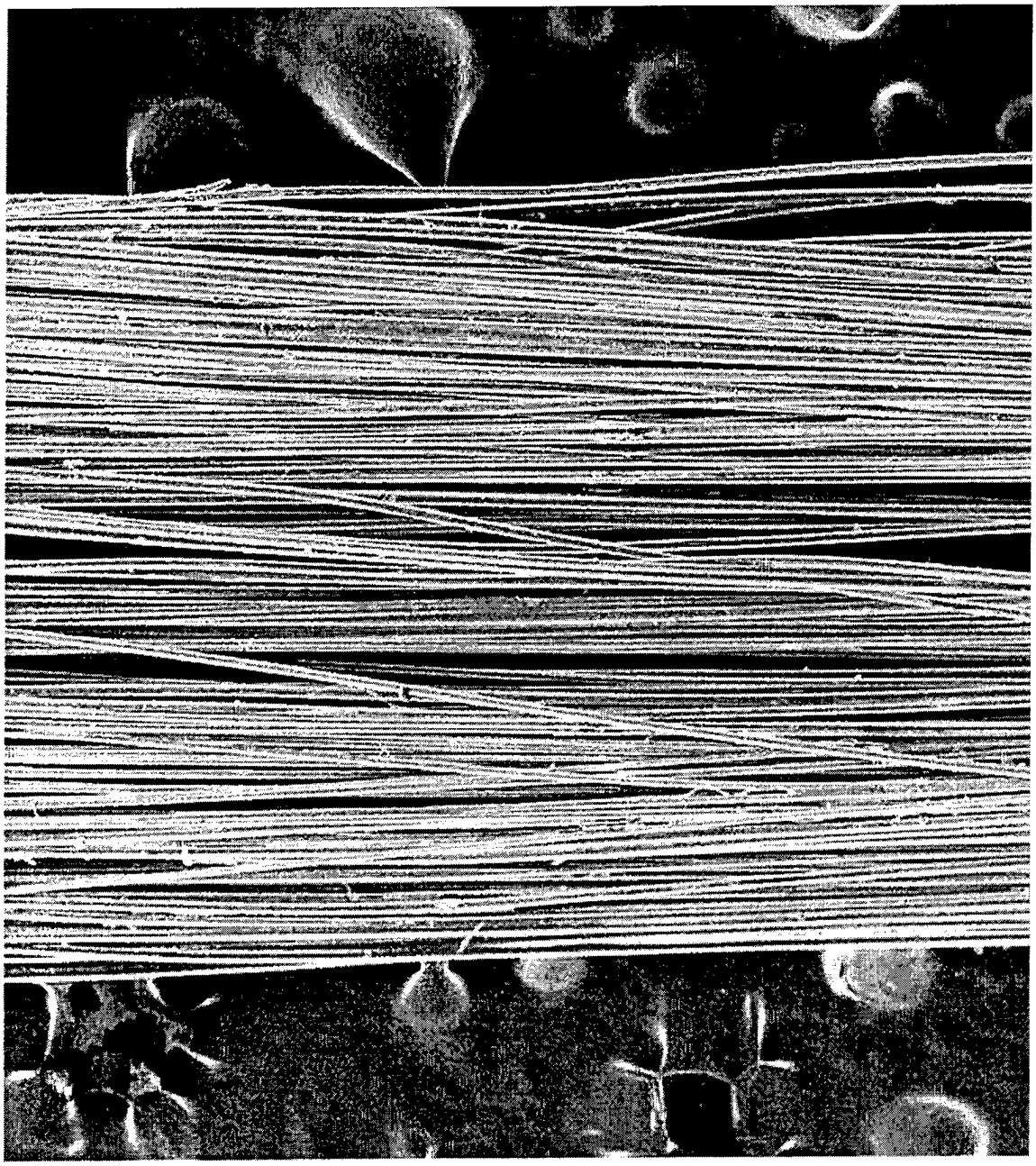

Figure 7. SiC Fiber Bundle Prior to Wetting Experiment

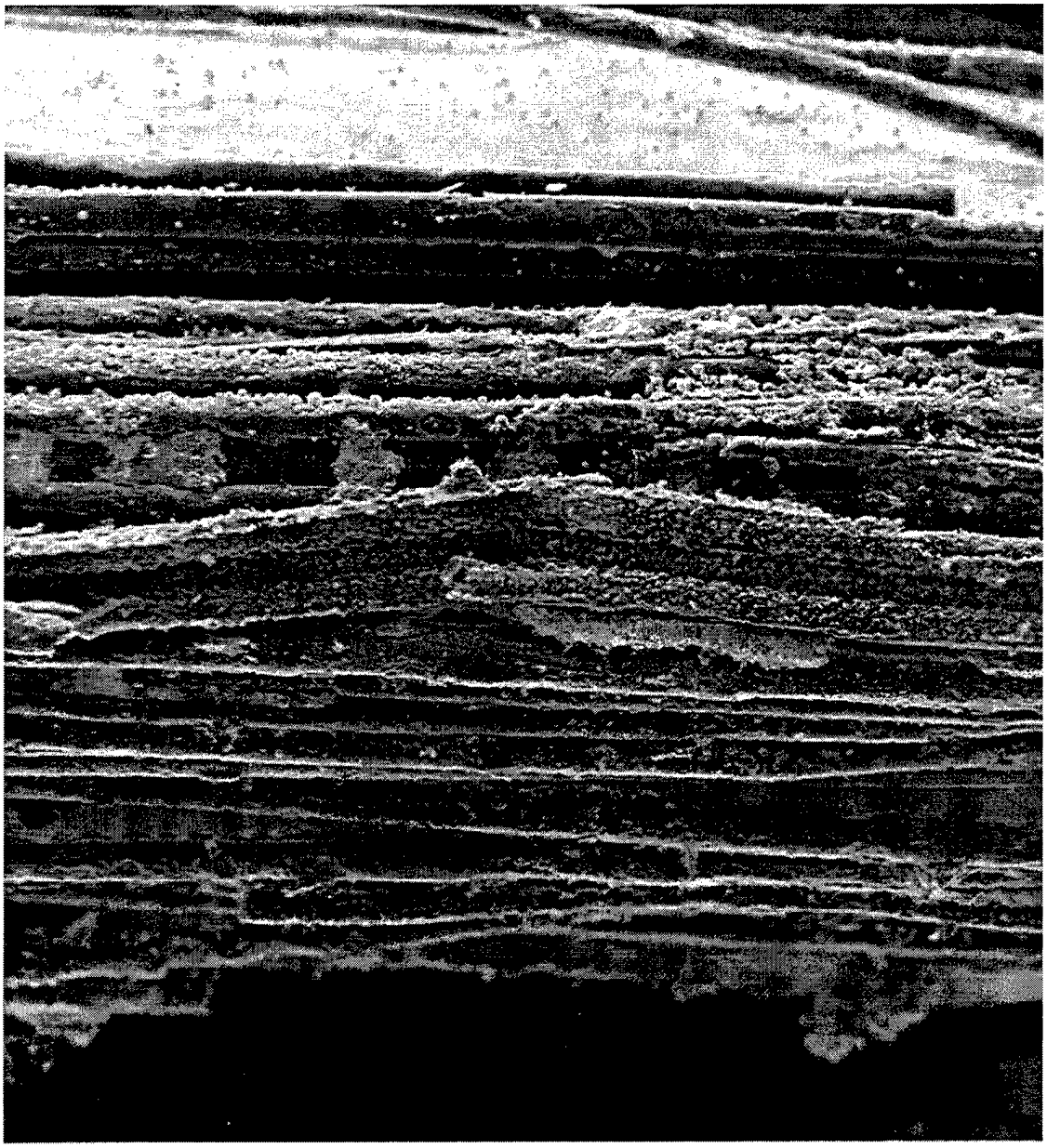

Figure 8. SiC Fiber Bundle After Wetting Experiment

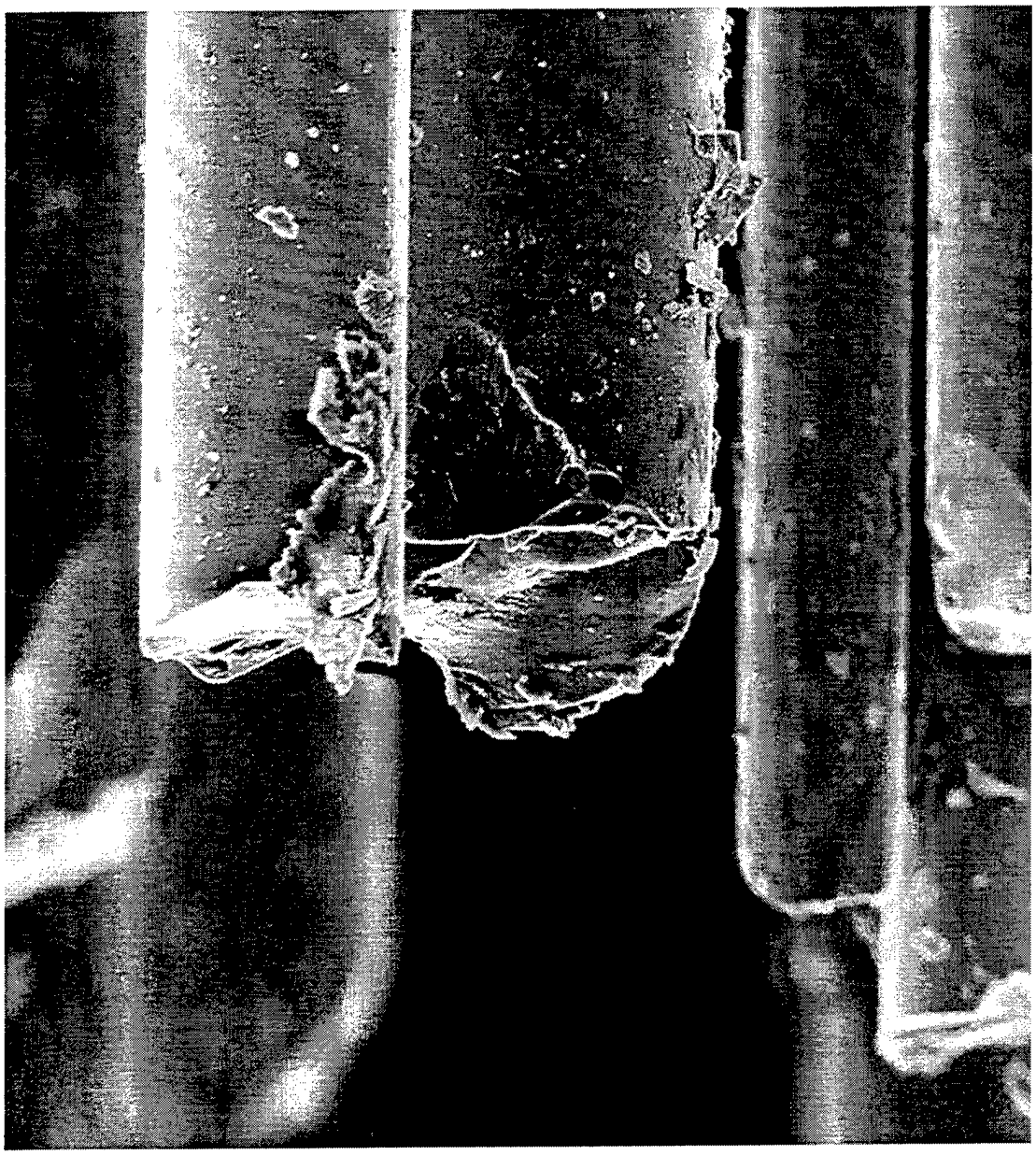

Figure 9. SiC Fiber Bundle End Prior to Wetting Experiment

Figure 10. SiC Fiber Bundle End After Wetting Experiment

The planar target design requires that ^{70}Ge lies flat on the substrate material to provide for an elliptical surface area. Experiment #6 indicated that ^{70}Ge uniformly coats the exposed flat surface of a foil composed of W. In addition, W is used as a Ge crucible indicating long term material compatibility [19].

Just as the name birdsnested suggests, this design uses a wire, with the appropriate diameter and length, that is randomly "balled up" to fit inside the target container. From experiments #3, #9, #12, #16, #17, and #18, it is apparent that a Mo wire substrate would form uniform coatings over the whole length of wire in the nest. See Figure 6.

The fibrous target is a substrate incorporating many fine wires or whiskers of a candidate material which could possibly increase surface area a thousand fold. Experiment #19 pointed to SiC as a candidate substrate material for this design, but later work indicates that Ge does not wet SiC. This may be attributable to non-uniform heating of the samples.

A porous foam substrate material, if uniformly coated, would increase surface area considerably. The foam is comprised of a wetable material that is manufactured in such a manner to increase the surface area by having pores throughout the material. SiC foam is found to have very high porosity that vastly increased the surface area. Based on findings in experiment #20, this foam seemed to be wet by Ge.

Once suitable substrate materials were determined, prototype second-generation targets were designed and tests were conducted on two. Careful thought and analysis must go into these designs to ensure Short diffusion paths without significantly reducing the amount of Ge available for ^{69}As production through ^{70}Ge (p, 2n) ^{69}As reaction.

III. TARGET DESIGN

In this section, the various criteria that are necessary to design functional RIB targets will be examined and four designs proposed. The geometry needs to be optimized in order to provide maximum RIB production, for specific driver beam energy, and a given energy dependence for the reaction cross section. In this case, ^{70}Ge (p, 2n) ^{69}As will be the reaction under consideration.

A. DIFFUSION OF NUCLEI THROUGH LIQUIDS

1. Diffusion Lengths and Coefficients

Of paramount interest is the length a RIB species can diffuse through target material before undergoing radioactive decay. Diffusion is defined as the process whereby particles of gases, liquids, or solids intermingle as the result of their spontaneous movement caused by thermal agitation and move from a region of higher to one of lower concentration. Even when relatively high production rates exist, the net yield will be adversely affected by slow diffusion. Equation 3.1 gives the average distance a radioactive atom may travel before decay.

$$Length = \sqrt{D \cdot \tau_{1/2}} \tag{3.1}$$

In the above equation, D is the diffusion coefficient and $\tau_{1/2}$ is the half-life of the species. The half-life of ^{69}As is 15.1 minutes.

Diffusivity, or atomic migration, is an important factor in the ability of a target to produce ions effectively. The higher the diffusion rate of a species, the better the yield. In this analysis, the self-diffusion of Ge in Ge will be used because there has been very little experimentation in the diffusion of ^{69}As from Ge [20].

An empirical form of self-diffusivity can be approximated as:

$$D = D_o e^{-\left(H_D/RT\right)} \tag{3.2}$$

Where D_o, H_D and R (Gas Coefficient) are constant and T is the temperature in Kelvin. H_D is the apparent activation energy for diffusion and, from empirical relationships can be evaluated using the following relationship for semi-metals (i.e. Ge) $H_D = 2.0 \cdot T_m^{1.15}$. The empirical form of self-diffusivity for a material at its melting point can be expressed [20]:

$$D_m = 3.5x10^{-6}\sqrt{\frac{T_m}{M}}\sqrt[3]{V_m} \ (\text{cm}^2/\text{s}) \tag{3.3}$$

T_m is the temperature of the material in Kelvin at the melting point. V_m is the atomic volume of the material at the melting point. M is the atomic mass of the material in AMU. When the above equations are combined, the resultant equation of self-diffusivities in liquid metals becomes:

$$D = \frac{3.5x10^{-6}\sqrt{\frac{T_m}{M}}\sqrt[3]{V_m}}{\sqrt{M}e^{-\left(\frac{H_D}{RT_m}\right)}}e^{-\left(\frac{H_D}{RT}\right)} \ (\text{cm}^2/\text{s}) \tag{3.4}$$

The diffusion length can be estimated from evaluation of Equations 3.1 and 3.4 and a maximum thickness of ^{70}Ge determined. From this approximation, the diffusion length was found to range from 1.8 mm (melting point) to 2.75 mm (current maximum operational temperature).

Alternatively, a hard-sphere model can be described as shown below. For Ge in Ge, this gives values for the diffusion length which range from 1.7 mm to 1.85 mm [20].

$$\eta = \frac{\pi}{6} \cdot \frac{N_{atoms}}{V} \cdot \varphi^3 \tag{3.5}$$

$$D = 4.9x10^{-6} \sqrt{\frac{T}{M}} \sqrt[3]{V} \frac{(1-\eta)^3}{\eta^{5/3}\left(1-\frac{\eta}{2}\right)} \tag{3.6}$$

Here η is the packing density of the atoms, V is the atomic volume, and φ is the effective hard-sphere diameter. Both theories suggest that the diffusion length is 1.8 mm at the melting point and increasing to ~2.3 mm at 1500°C. Therefore, if the diffusion of As in Ge is similar to Ge in Ge, the maximum thickness for the coating of ^{70}Ge should be on the order of 1 mm or less.

2. Calculation of Fractional Release

To qualify the fraction of the radioactive material released from the target prior to decay the diffusion equation can be solved for spherical, cylindrical and planar geometry's. This fraction can be expressed as a function of a dimensionless parameter, α.

$$\alpha = \frac{\bar{\tau} \cdot D}{a^2} = 0.693 \frac{\tau_{1/2} \cdot D}{a^2} \tag{3.7}$$

where $\bar{\tau}$ is the mean lifetime of the RIB species and a is the characteristic dimension of the target material. For spheres (droplets), a is the radius, for a plane (foil), a is ½ the thickness, and for cylinders (thick fiber coating), a is the

coated fiber radius. The fraction of the RIB species released from the liquid before decay can then be expressed as

Foil: $$F_r = \sqrt{\alpha}\tanh\left(\frac{1}{\sqrt{\alpha}}\right) \tag{3.8}$$

Fiber: $$F_r = 2\sqrt{a}\frac{I_1\left(\frac{1}{\sqrt{a}}\right)}{I_0\left(\frac{1}{\sqrt{a}}\right)} \tag{3.9}$$

Sphere: $$F_r = 3\sqrt{\alpha}\left[\coth\left(\frac{1}{\sqrt{\alpha}}\right)-\sqrt{\alpha}\right] \tag{3.10}$$

Where $I_s(1/\sqrt{\alpha})$ is the modified Bessel function of the first kind of order s [21].

When the planar analysis is used to approximate release from the first generation HRIBF liquid target with D from section 1, $F_r > 30\%$ is obtained. The observed fractional release from this target is, however, approximately an order of magnitude less [13]. See section I.D. This suggests that D is actually much smaller than the theoretical value derived in the previous section for Ge diffusing in Ge. It maybe that As diffusion is slower than Ge diffusion or diffusion is limited by an oxide layer on the Ge surface as suggested by ISOLDE [22]. In both cases, reducing the targets diffusion path, distance a particle must travel before desorbing, effectively increases the targets surface area, which should overcome these limitations

B. ENERGY LOSS OF IONS IN MATTER

The optimal thickness of a target is directly related to how far the proton beam will travel in the material before falling below the regime of useful

production. Several processes account for energy loss rate (dE/dx) during target penetration. Direct collisions between ions and nuclei, excitation of bound electrons, and charge exchange processes between ions and atoms [23] are the major processes involved and are summarized in Equation 3.10.

$$\left(\frac{dE}{dx}\right)_{\text{total loss}} = \left(\frac{dE}{dx}\right)_{\text{nuclear}} + \left(\frac{dE}{dx}\right)_{\text{electronic}} + \left(\frac{dE}{dx}\right)_{\text{charge exchange}} \tag{3.10}$$

The largest term is based on excitation of electrons and can be expressed as

$$\left(\frac{dE}{dx}\right)_{\text{electronic}} = \frac{4\pi Z_1^2 e^4}{mv^2} B \tag{3.11}$$

where B is a measure of the penetration through the electron shells, Z_1 is the atomic number of the incident beam (Z_1=1), m is the mass of an electron, v is the velocity of the electron, and e is the charge of an electron [23].

The computer code SRIM was used to make calculations of the rate of energy loss per unit length of target material and uses the $(dE/dx)_{electronic}$ and $(dE/dx)_{nuclear}$ terms. The $(dE/dx)_{charge\ exchange}$ accounts for a small percentage of the total (dE/dx) and will be neglected. This code can also be used to calculate dE/dx directly. Figure 11 shows dE/dx versus proton beam energy in pure ^{70}Ge. SRIM is actuality is a group or programs capable of determining the stopping power and range of ions in the 10eV to 2 GeV/amu region. SRIM uses a quantum mechanical treatment of ion-atom (incident beam – target material) collisions Using Monte-Carlo calculational techniques; SRIM can evaluate compound targets composed of up to eight layers of different target materials. Figure 12 shows an example of the data input page. A full description of the calculations and physics can be found in the tutorial book "*The Stopping and Range of ions in Solids*" by J.F. Zeigler, J.P. Biersack and U. Littmark, Pergamon Press, New York, 1985 [24].

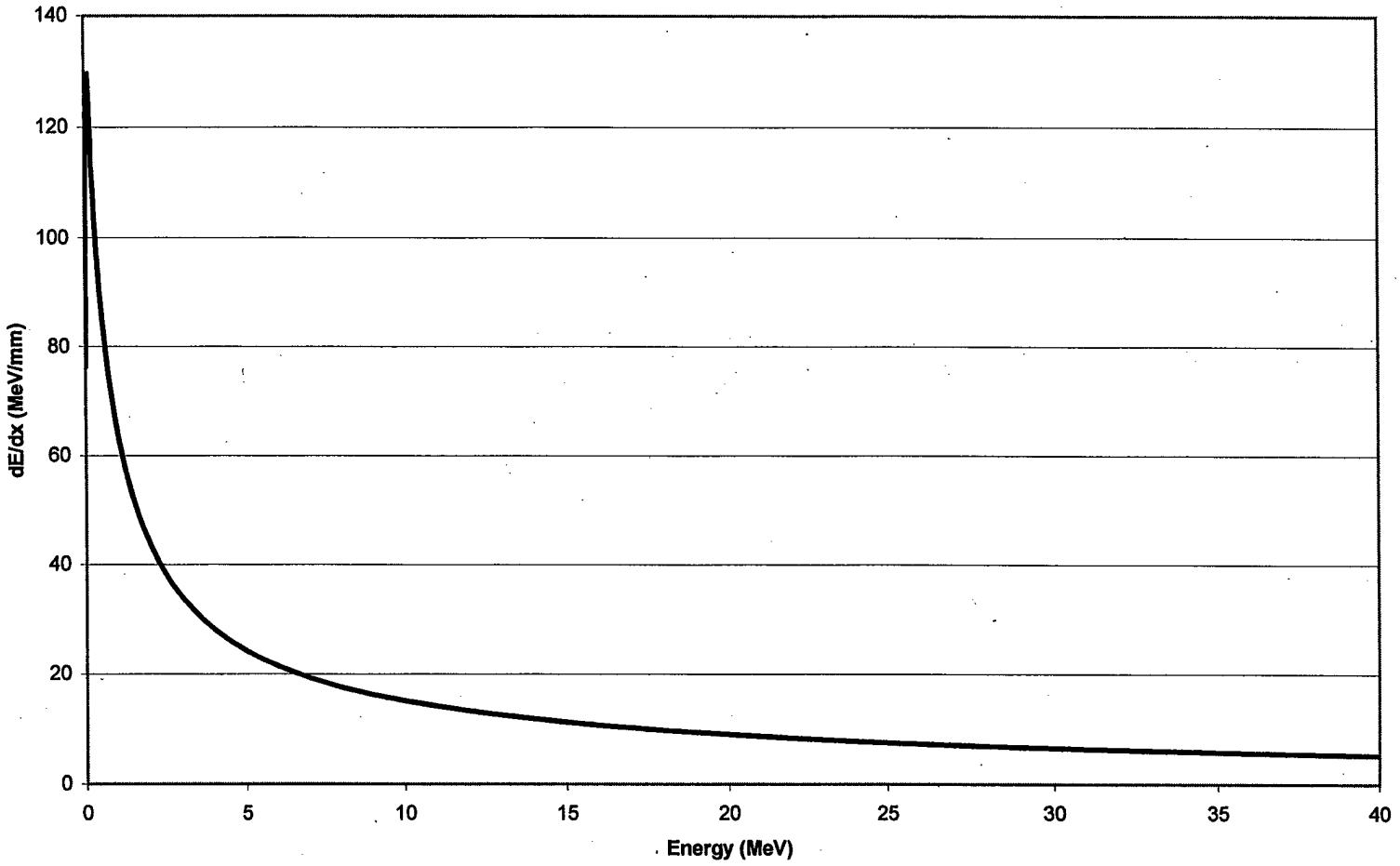

Figure 11. dE/dx versus energy E in pure ^{70}Ge bombarded by protons calculated by SRIM.

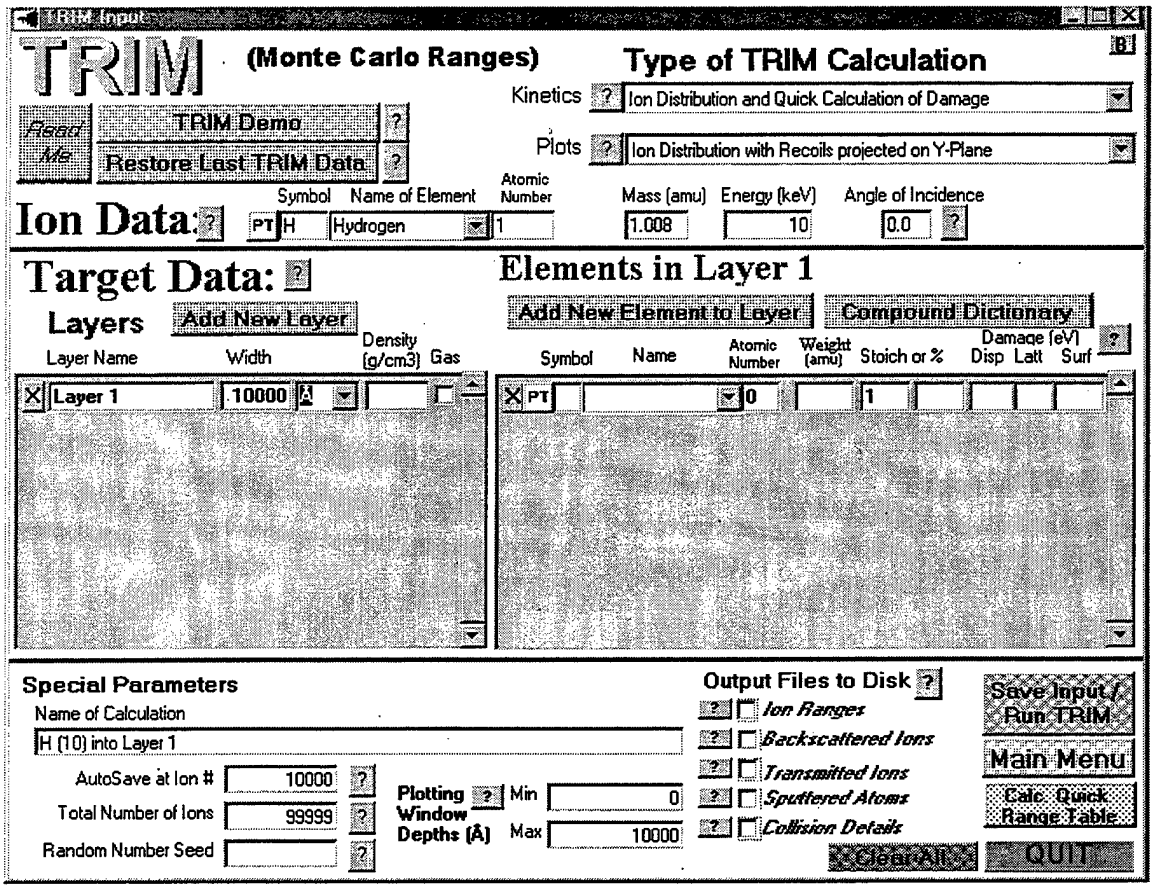

Figure 12. Example of TRIM Data Input Page.

In order to determine optimum target thickness for the composite targets proposed in this thesis, proton beam energy as a function of penetrating depth into the target must first be calculated. If the target is too thick, it will be heated excessively by the Bragg peak, shown in the dE/dx versus E curve (Figure 11), which will reduce the total beam current the target can stand. If the target is too thin, RIB production will be compromised as useful beam exits the target. Fortunately, SRIM can handle energy loss in composite targets and was used to calculate beam energy versus depth curves for our proposed composite targets. The curves will be used in the next section to compute total production rates of each of these targets. The detail of each configuration is given in the figure captions and in section III.F. Figures 13, 14, 15 and 16 show the proton energy loss curves calculated from SRIM for the four concept targets.

C. CALCULATION OF THE RATE OF PRODUCTION FOR RIB ATOMS

A cross section is a convenient means of quantifying the rate at which a reaction will proceed and is widely used in physics and chemistry. The cross section has units of area and can be viewed as the geometrical cross section of each target particle such that if a projectile particle strikes within this area the reaction proceeds. To illustrate this concept, refer to Figure 17. The concept of a cross section can be expressed mathematically in a thin slab of collision gas as

$$dR = I \sigma n dx \tag{3.12}$$

The rate at which the reaction proceeds (dR) depends on the initial number of target atoms per unit volume (n), the flux (I) of projectile particles and the cross section (σ) [25]. Ge was chosen as the target material because of its comparitively large cross section for reactions generating ^{69}As by proton bombardment. Figure 18 shows a collection of nuclear cross section data points for the ^{70}Ge (p, 2n) ^{69}As reaction as a function of beam energy [26]. Figure 19

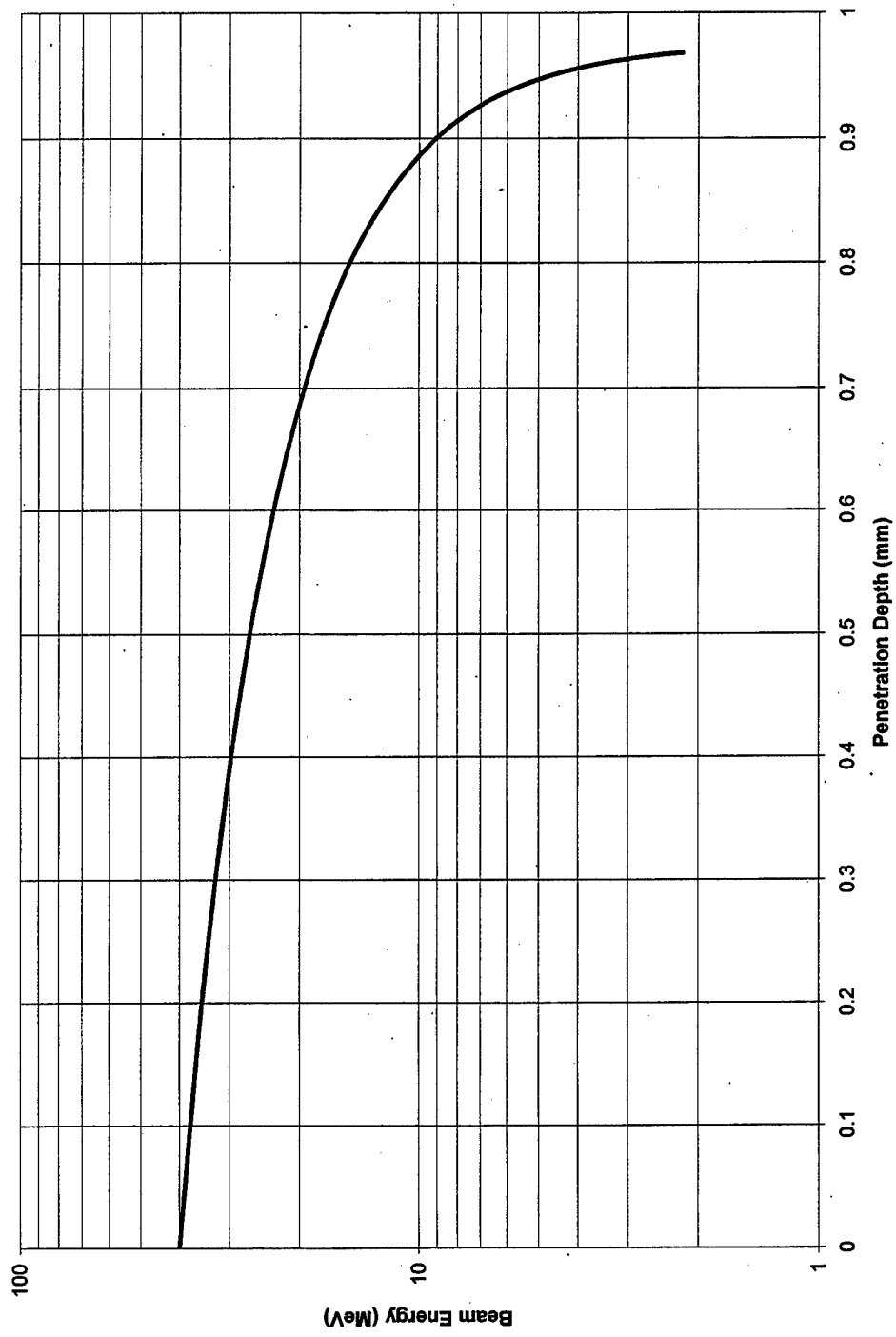

Figure 13. Energy remaining in a proton beam as a function of penetration depth calculated from SRIM for Planar Target consisting of 50 micron W window and 0.8 mm ^{70}Ge Layer traversed at incidence angle of 77° by 42 MeV proton beam.

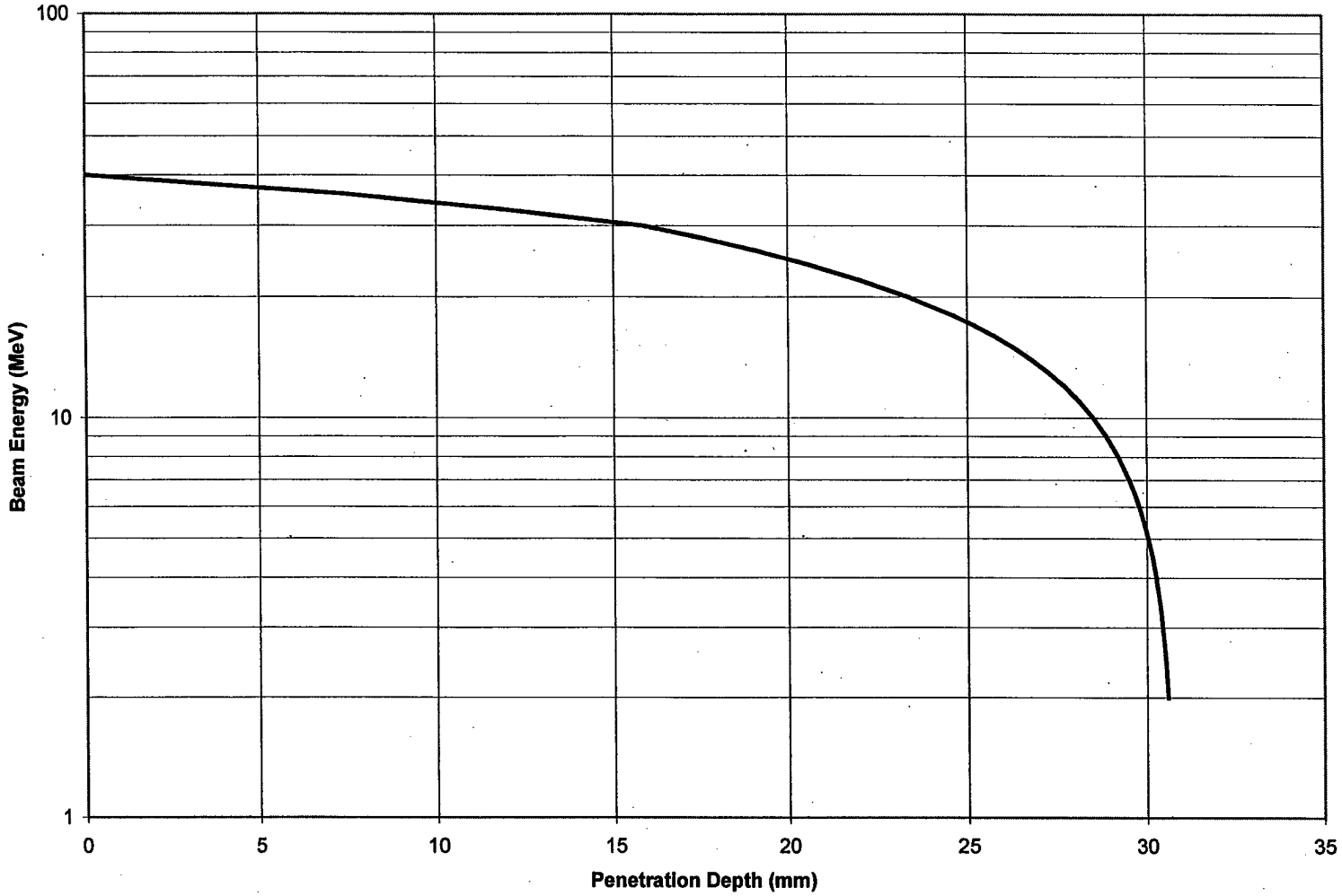

Figure 14. Energy remaining in a proton beam as a function of penetration depth calculated by SRIM for Birdsnested Target consisting of 1.0 mm graphite window and 25.0 mm ^{70}Ge+250 μm Mo Wire bombarded by 42.0 MeV Proton beam.

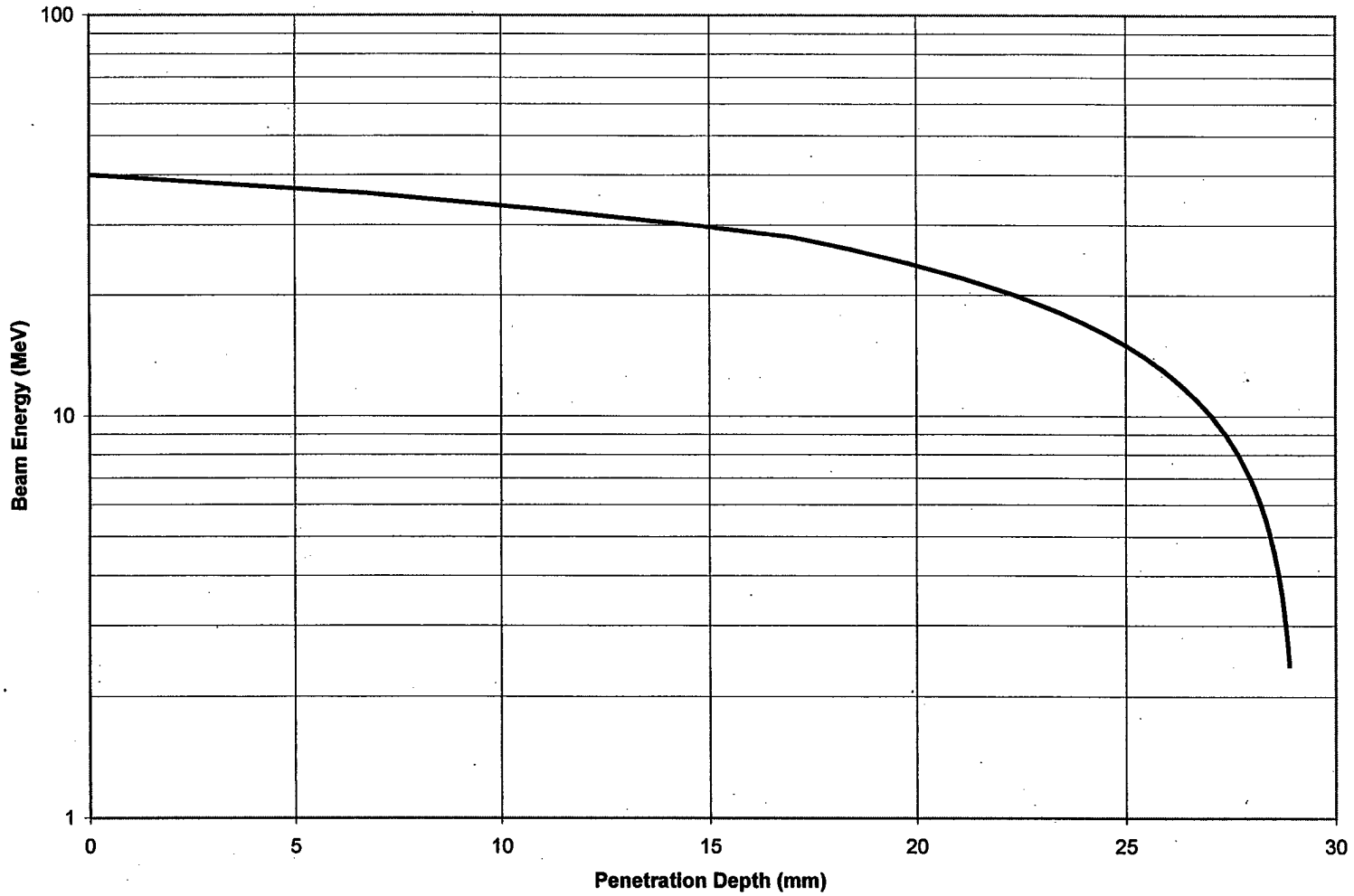

Figure 15. Energy remaining in a proton beam as a function of penetration depth calculated by SRIM for SiC Fibrous Target consisting of 1.0 mm graphite window and 25 mm ^{70}Ge+SiC Weave [85% porous] bombarded by 42.0 MeV Proton Beam. SiC weave is a 25 cm x 1 cm piece which is folded into the target container.

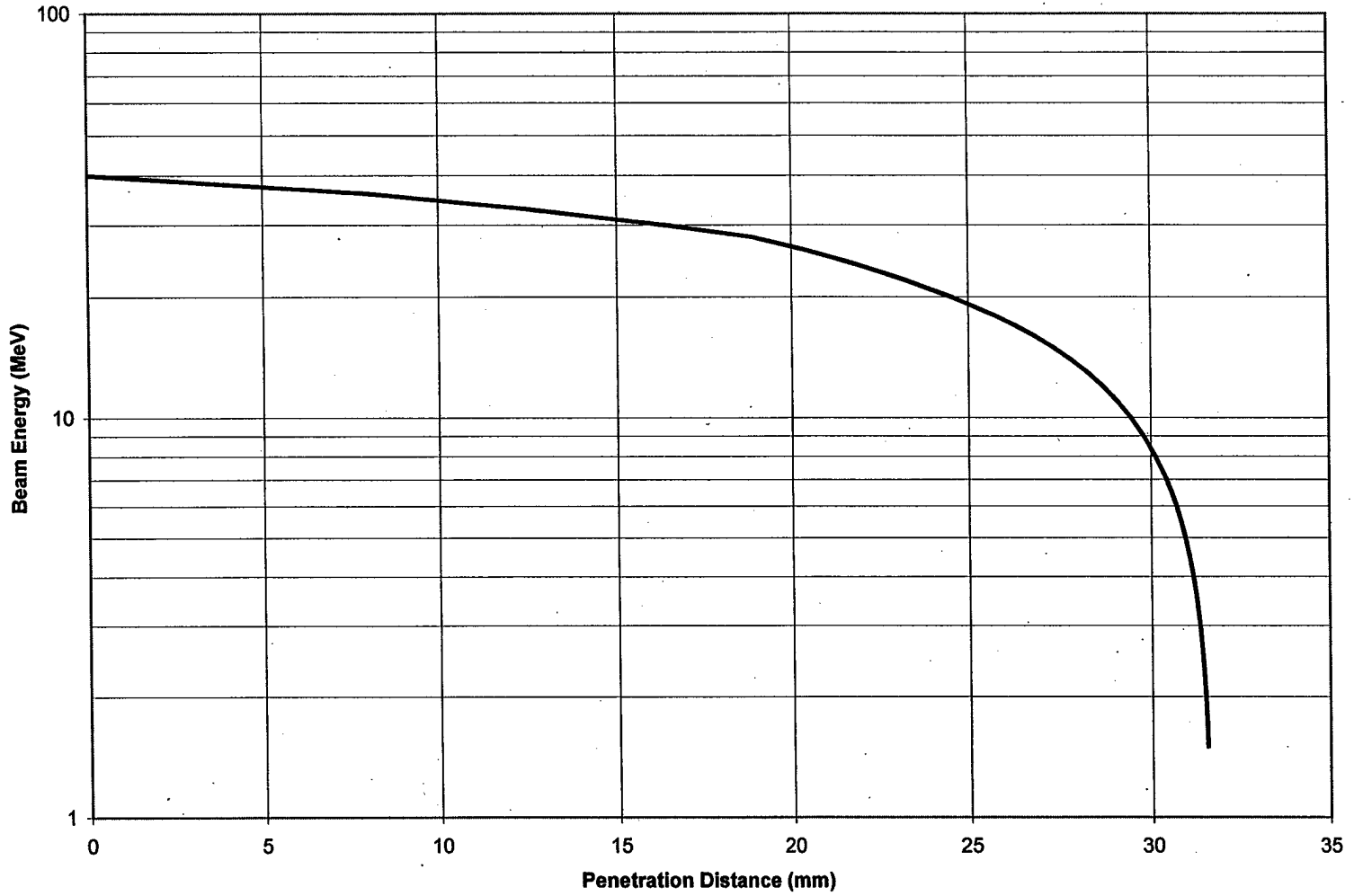

Figure 16. Energy remaining in a proton beam as a function of penetration depth calculated from SRIM for SiC Foam Target consisting of 1.0 mm graphite window and 25 mm ^{70}Ge+SiC foam of 88% porosity bombarded by 42 MeV proton beam.

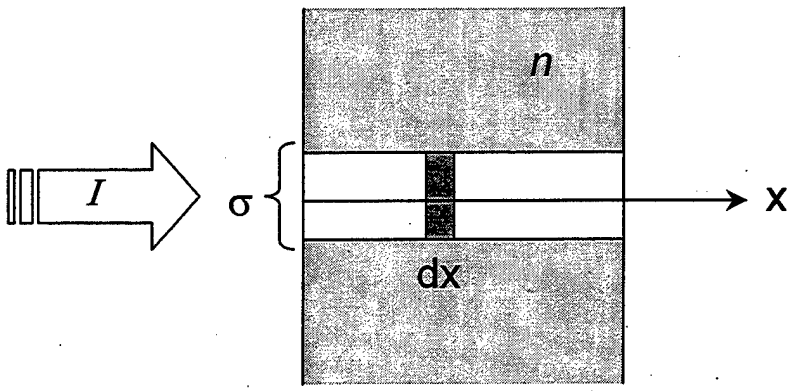

Figure 17. Illustration of the cross section and current interaction during target penetration.

shows Figure 18 superimposed over the dE/dx versus E plot for pure ^{70}Ge calculated in the previous section. It becomes clear that by having about 15 MeV of energy exit from the target, heating power density is significantly reduced and ion production is not adversely affected.

In order to determine the total rate of production of ^{69}As, we must fold the cross section versus energy data into the proton energy versus depth in the target curve calculated in the previous section. Since Equation 3.12 is a general representation of the change in the rate of production per unit length we can integrate it and by change variables we get:

$$R = \int I\,\sigma\,n\,dx = \int I\,\sigma(E)\,n\,dx = \int I\,\sigma(E)\,n\frac{dx}{dE}\,dE \qquad (3.13)$$

This leads to:

$$R = \int_{E1}^{E2} I\,n\,\sigma(E)\left(\frac{dE}{dx}\right)^{-1} dE \qquad (3.14)$$

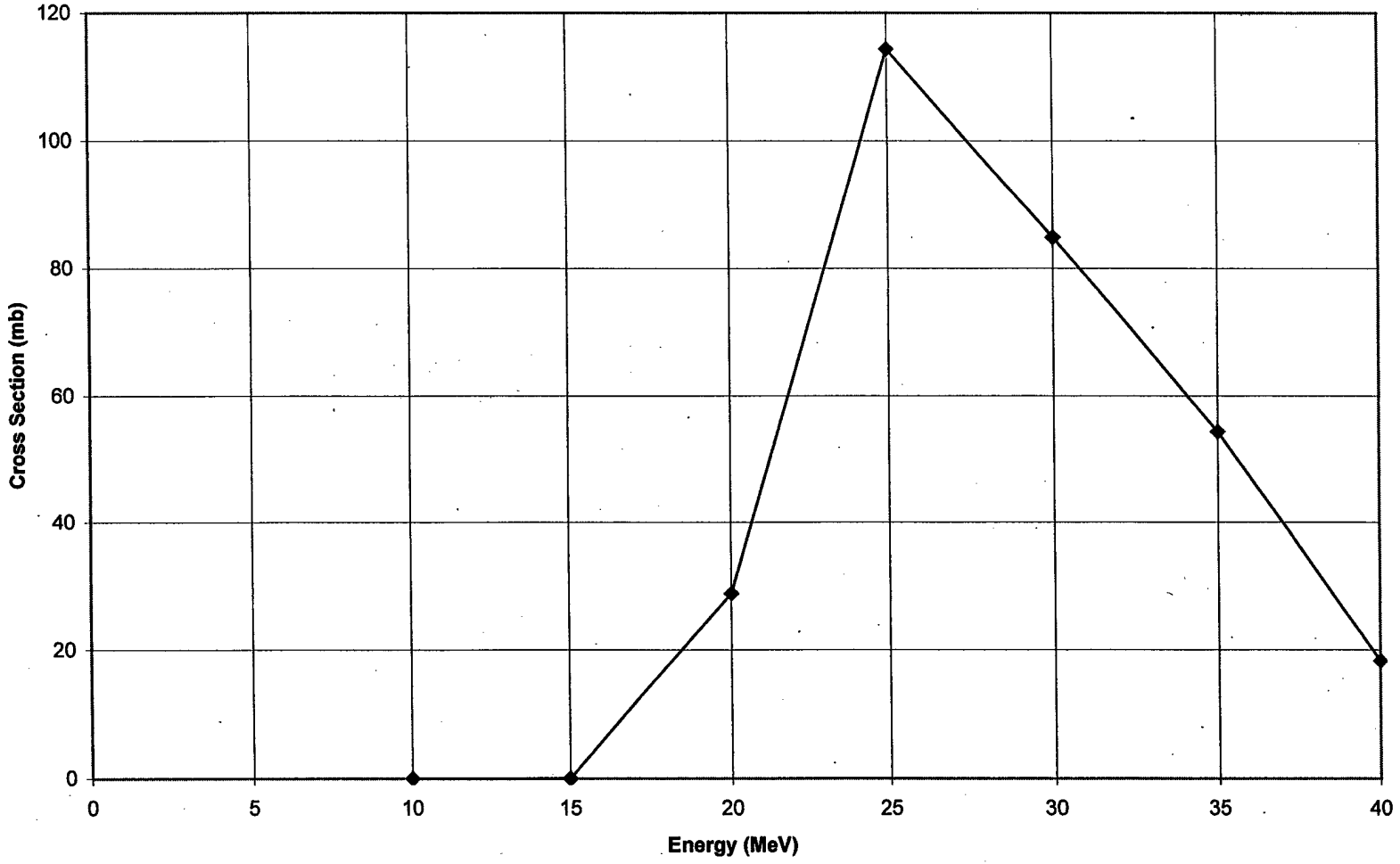

Figure 18. Nuclear Cross Section for ^{70}Ge (p,2n) ^{69}As Reaction vs. incident proton energy

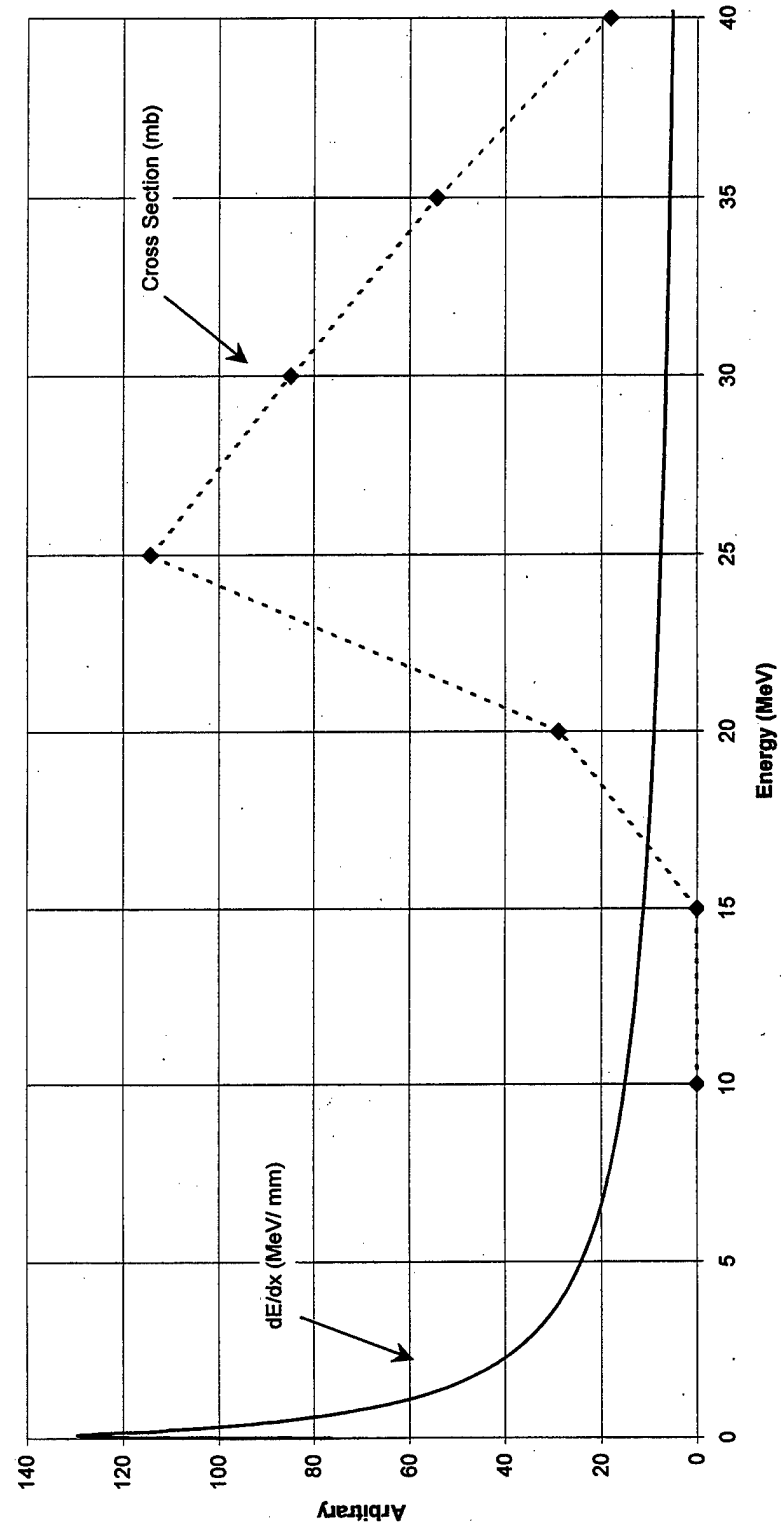

Figure 19. Figure 18 Superimposed over dE/dx Versus E Plot for ^{70}Ge.

Where E_1 is the incident beam energy and E_2 is the exit energy. Equation 3.14 represents the total number of atoms that are formed per second. As the cross section for the nuclear reaction is increased, the overall production rate of the desired species will also increase. As dE/dx increases, the production rate of the species will decrease. Production rates for the ^{70}Ge (p, 2n) ^{69}As reaction are calculated based on 1.0 MeV increments and are done so using the RADBEAM2 computer code which numerically solves Equation 3.14 [27]. Figures 20 through 23 show the resulting total production rates for ^{69}As as a function of incident beam energy accounting for degradation through the graphite entrance window for each of the four candidate designs. These results coupled with those of the previous two sections will determine what the characteristic thickness will be for each design and used to determine the effective TIS efficiency during operation.

D. DETERMINATION OF THE LIQUID COATING THICKNESS FOR CANDIDATE TARGETS

The basic design of each of the candidate target proposed in this thesis involves a liquid metal coating a solid substrate to reduce the effective diffusion length which also increases the surface area of the target. Calculations were conducted to determine the coating thickness. Each of the four candidate target configurations will be considered.

The planar target scheme is based on distributing the beam power over a thickness = 51 μm W horizontal window. The dE/dx versus E plots calculated in the previous section show that a thickness of 3.2 mm of Ge results in ~15 MeV exit beam energy when the incident beam has 42 MeV. The geometry of this target has the incident beam entering the target on an axis 13° below the horizontal. Figure 24 shows the target configuration.

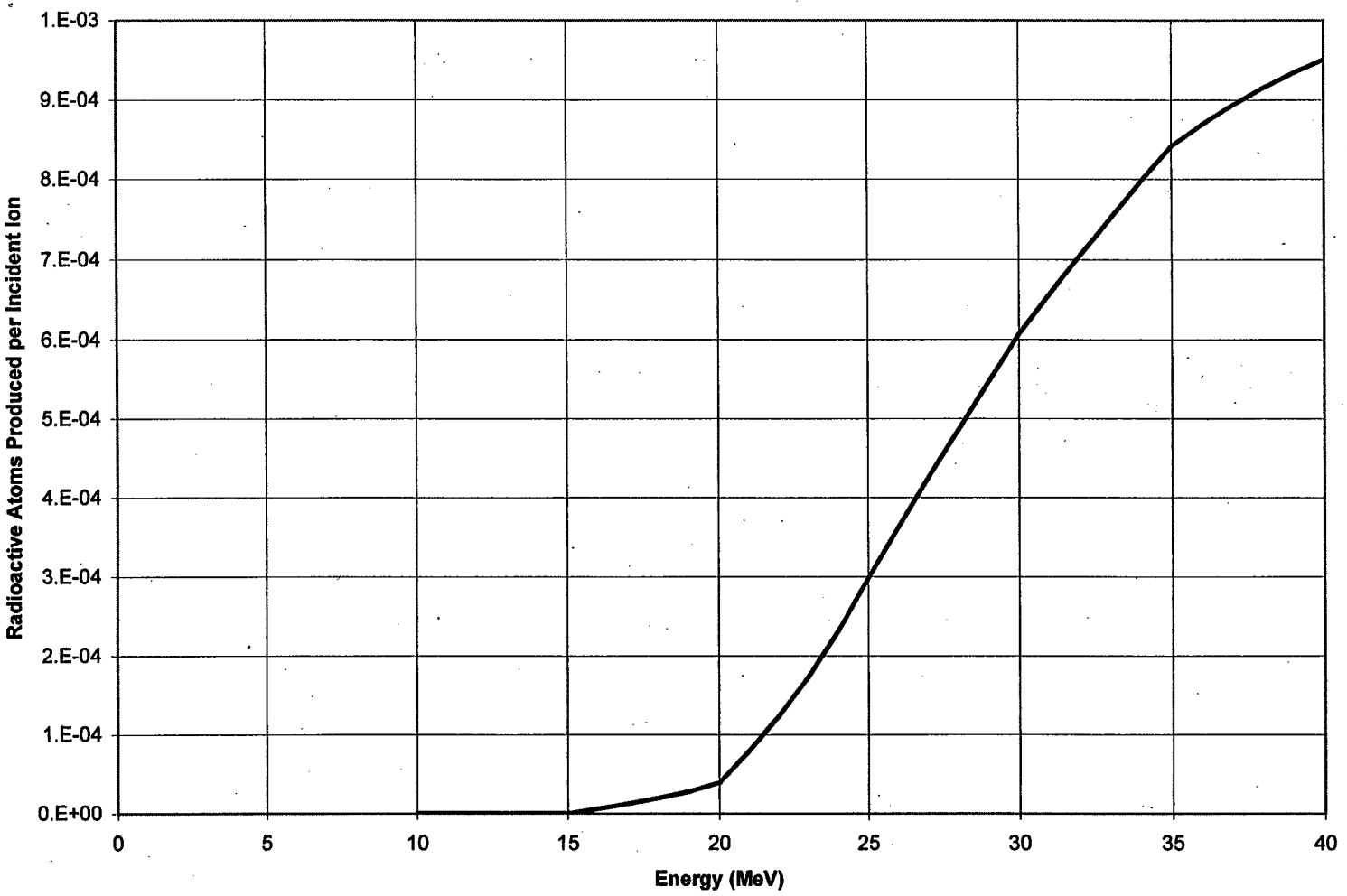

Figure 20. Production Curve of ^{70}Ge (p, 2n) ^{69}As Reaction for Planar Target consisting of 50 μm W window and 0.8 mm ^{70}Ge Layer. 42 MeV proton beam of 77° incidence calculated from RADBEAM2.

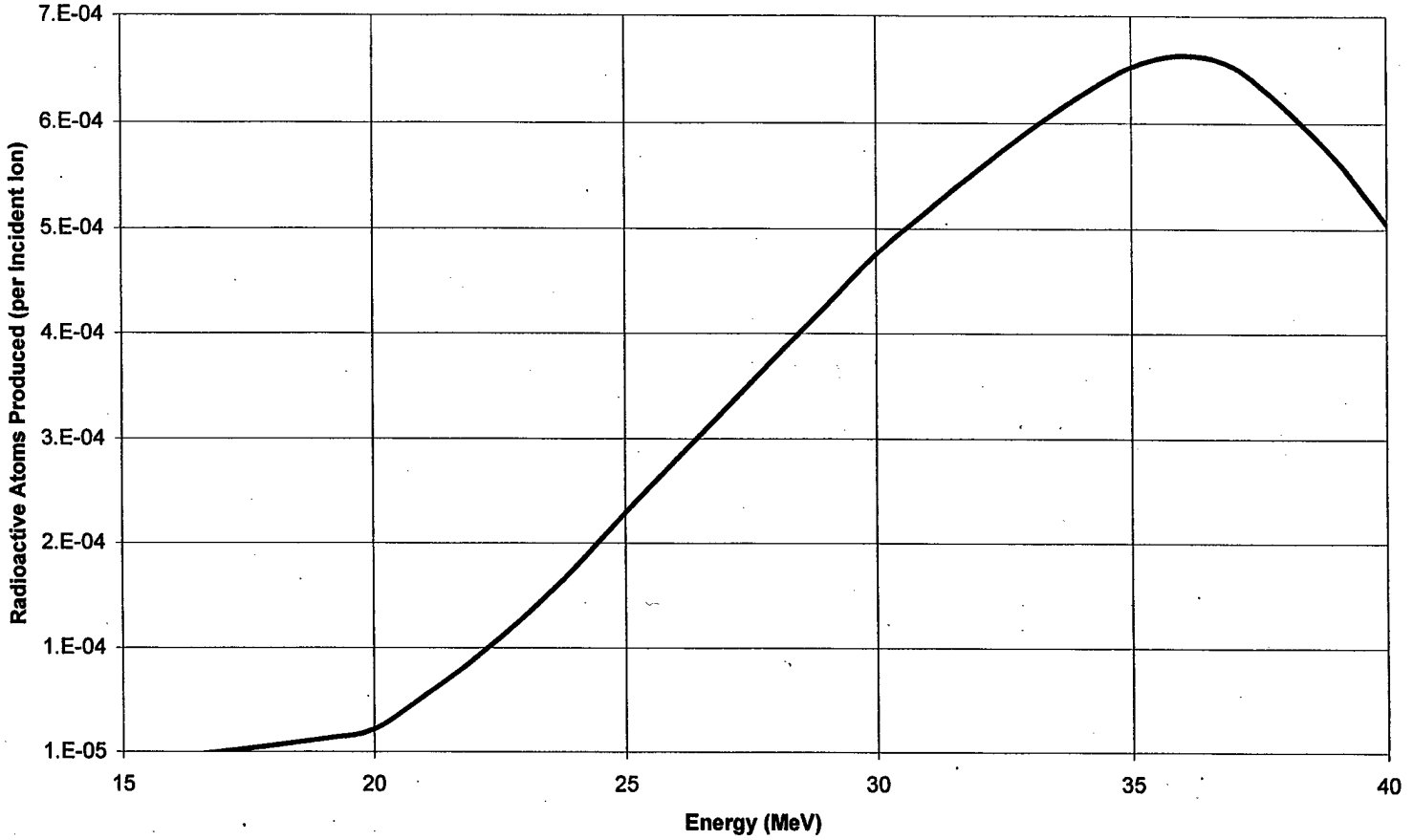

Figure 21. Production Curve of ^{70}Ge (p, 2n) ^{69}As Reaction for Birdsnested Target consisting of 1.0 mm graphite window and 25 mm ^{70}Ge+250 μm Mo Wire calculated by RADBEAM2.

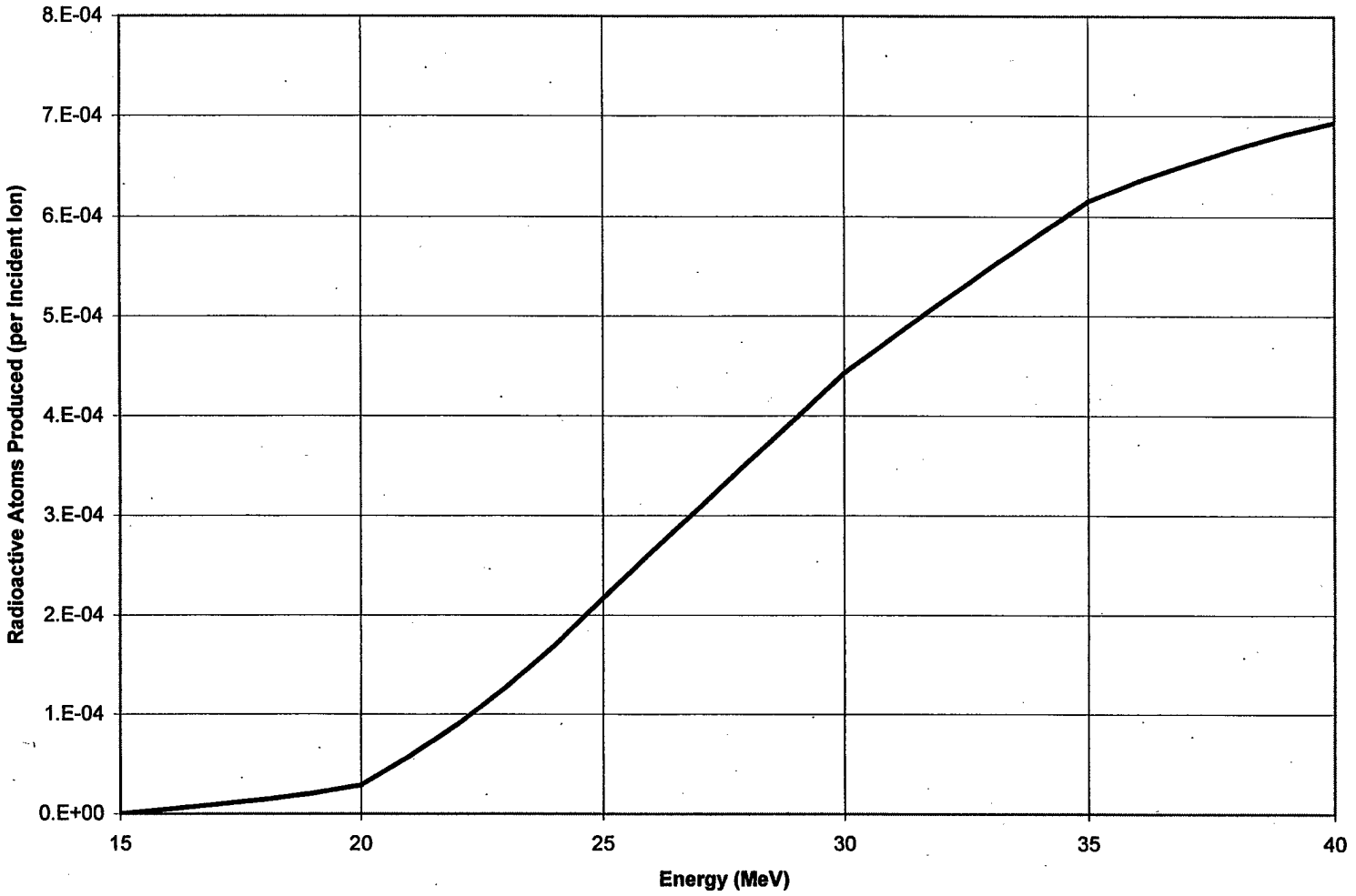

Figure 22. Production Curve of ^{70}Ge (p, 2n) ^{69}As Reaction for SiC Fibrous Target consisting of 1.0 mm graphite window and 25 mm ^{70}Ge+ SiC Weave [85% porous] calculated by RADBEAM2. SiC weave is a 25 x 1 cm piece of material that is folded into the target container.

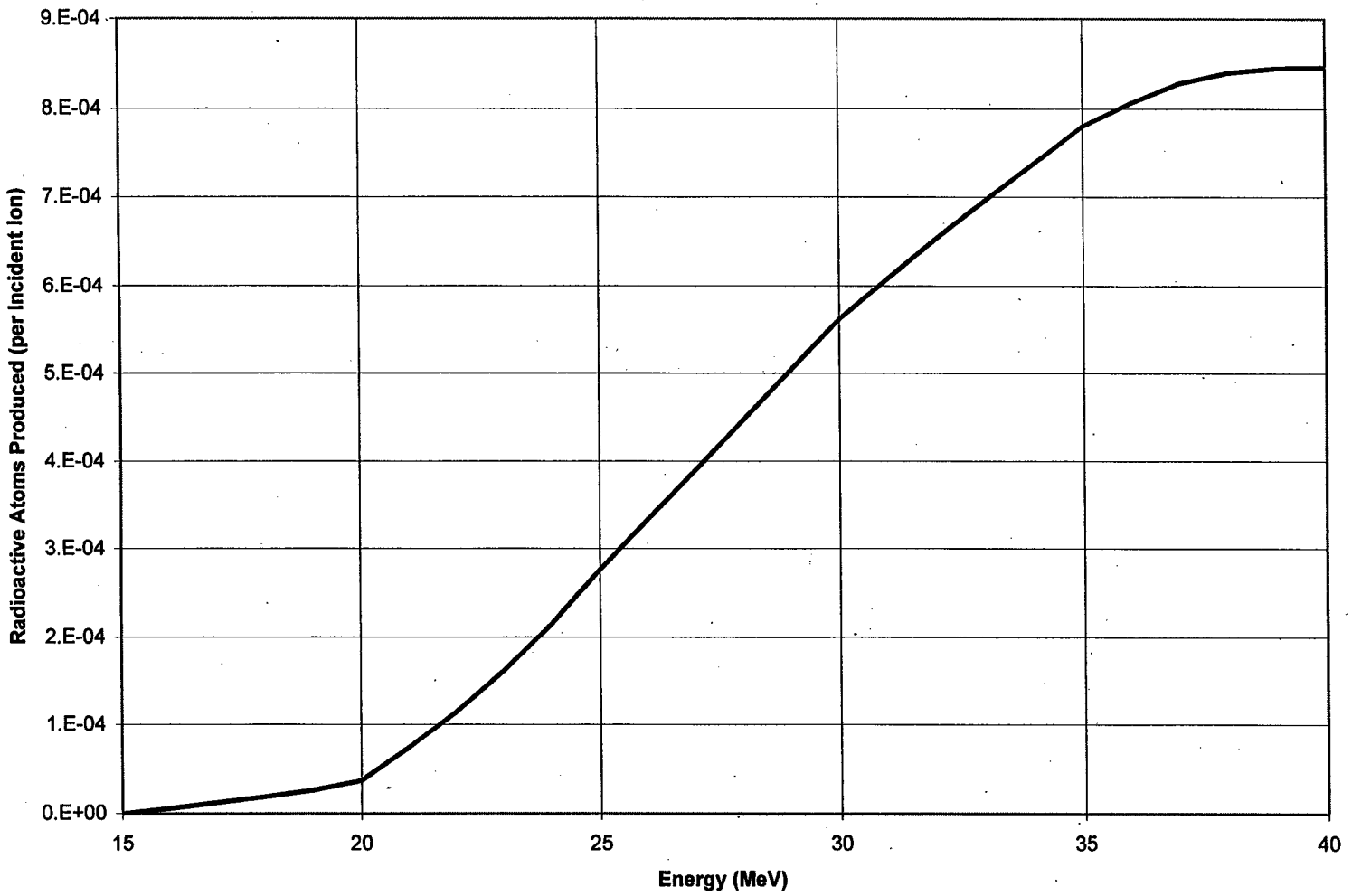

Figure 23. Production Curve of ^{70}Ge (p, 2n) ^{69}As Reaction for SiC Foam Target calculated from RADBEAM2.

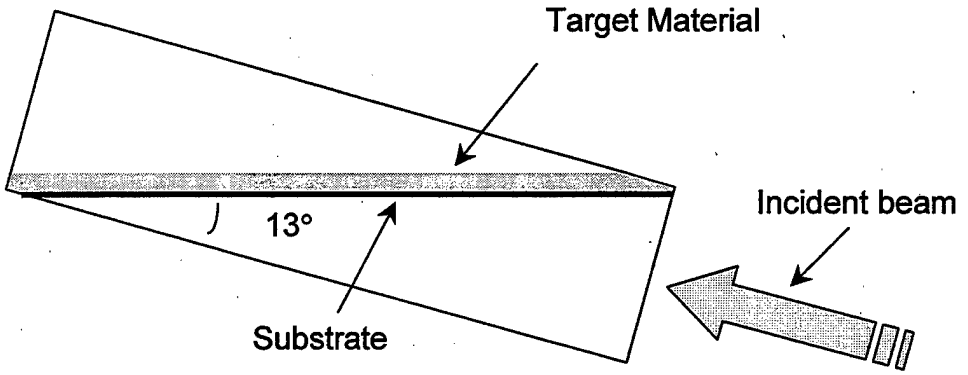

Figure 24. Planar Target Configuration

To determine the distance the beam will travel through the target material Equation 3.15 is used to account for the inclined incident beam.

$$\sin(13^\circ) = \frac{\text{Target Thickness}}{\text{Distance Beam Travels in Target}} \qquad (3.15)$$

Solving for the target thickness, a coating of 0.8 mm is required. Thus, enough Ge will be added to the target to achieve this coating thickness.

The birdsnested target design requires a Ge coating on fine Mo wire such that the 42 MeV incident beam will exit with ~15 MeV. The procedure to determine this coating thickness is described. First, a nominal thickness (about one diameter of a wire ~ 250 μm) was chosen. Second, the mole ratio of the Ge to substrate was fixed to be at least 9:1. Third, porosity needed to be between 85 and 90% to allow for product atoms an avenue to effuse. Fourth, the average density of the target was calculated, see section III.B. These numbers were then input into the SRIM program and the average exit energy was calculated. Target parameters, such as wire diameter, were iteratively changed one at a time until optimum exit energy was found. For this target, 82 cm of 250 μm Mo wire with a

Ge coating of 250 μm was determined. The exit beam energy was determined to be 17.5 MeV.

The Ge coated SiC fiber target required the same procedure employed above for the birdsnested target. A weave of commercially available SiC fiber composed of 15 μm strands was used for these experiments. The surface area of the SiC weave is taken from the product sheet. We determined that a 25 cm x 1 cm SiC fibrous sheet would meet design criteria. With a uniform coating thickness of 9.6 μm the exit beam energy would be 19.2 MeV. Later work showed that the SiC Fiber is not wet by Ge (see section IV.2).

The final highly pervious target was the SiC foam based target. When dealing with foam material, the surface area is often given in relation to the weight of the material being used (i.e. 1000 cm^2 per gram). The same procedure as in the birdsnested target was used in finding the characteristic parameters for the target. For this target, a Ge coating of 41 μm would result in a porosity of 87% and exit beam energy of 14.42 MeV.

E. THE TARGET HOLDER DESIGN

For maximum usability, we designed a single target holder that could be easily adapted to any of the four different target configurations. A baffle to create a vapor pressure barrier between the target and the ion source and to allow for recirculation of the Ge was incorporated into the target holder. Since it was not clear exactly what the optimum temperature the baffle needed to be, a secondary ohmic heater was added to the baffle-cooling fin to provide some measure of control over this temperature.

The baffle is introduced to allow target material heating to temperatures where the vapor pressure is greater than 10^{-4} Torr, while permitting the ion source to be maintained at pressures below 10^{-4} Torr. Ion source efficiency is drastically reduced when the source pressure rises above10^{-4} Torr [28] because ion losses through neutralization becomes a factor. Ge escaping into the vapor

transfer tube must first pass through the cooled baffle allowing condensation and return to the target container.

Figure 25 shows the vapor pressure curve for Ge as a function of temperature as computed by the HSC Thermodynamic Equilibrium Code [29]. Data from the first generation targets suggests that 1560°C is the maximum operating temperature of the target without any baffling. The Vapor pressure of Ge would reach 1.0×10^{-1} Torr at the upper limit, higher than the 10^{-4} Torr required at the ion source.

The length of the target holder was chosen solely to accommodate the planar target. This target holder is 2.5 cm long. The inner diameter of the holder is the size of a slightly defocused beam (1.3 cm maximum). Ta was used as the target holder crucible primarily because of its performance in past designs, machinability, welding characteristics, and material integrity at high temperatures. Figure 26 is a photograph of the target assembly. The assembly is composed of the target holder, transport tube for the radioactive species and a Xenon (Xe) gas line. The target container discussed in Chapter II.D.5 slips inside the target holder as in Figure 27. Each design discussed below fits into the target container.

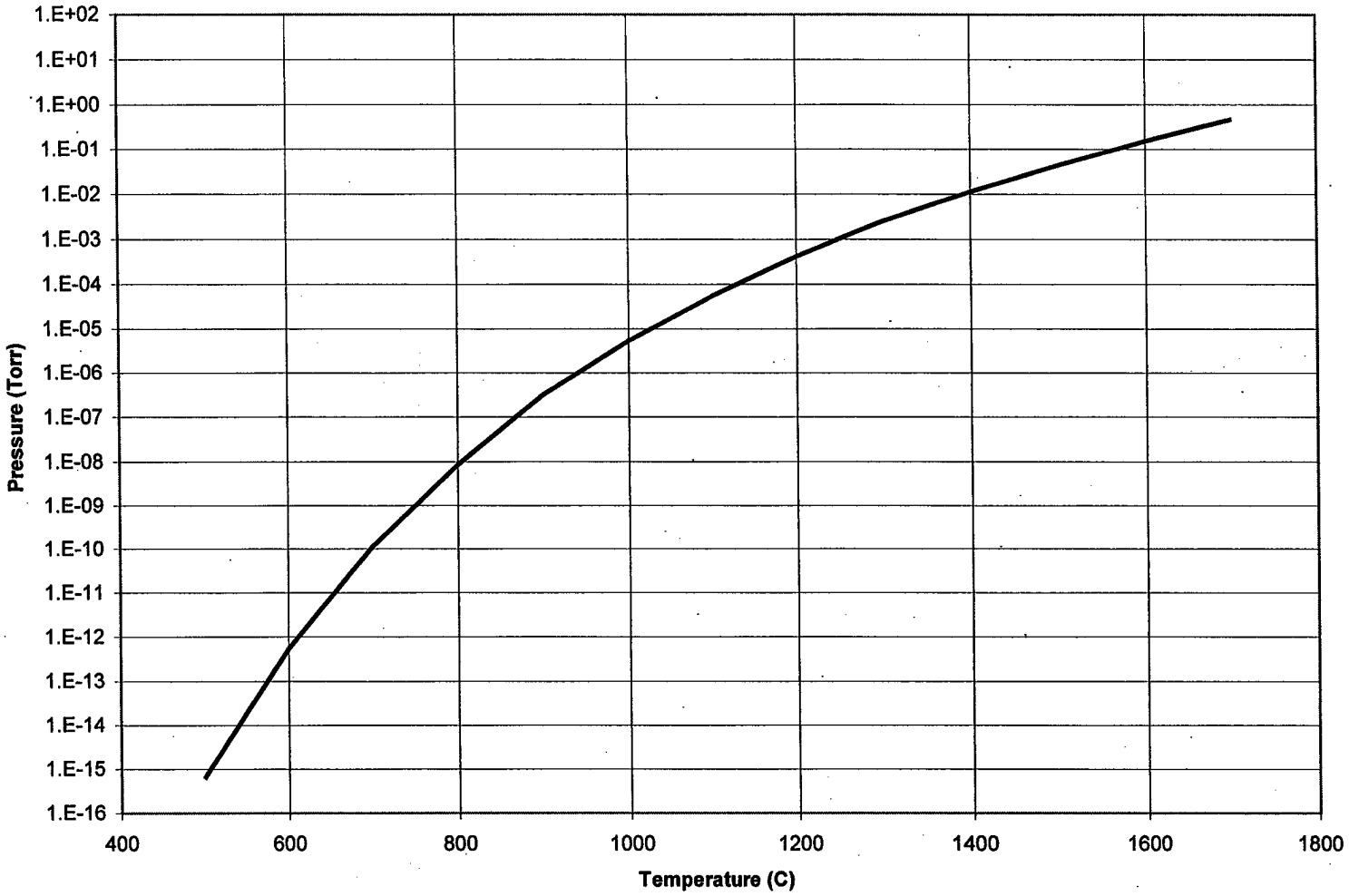

Figure 25. Vapor Pressure of Ge based on HSC Calculations.

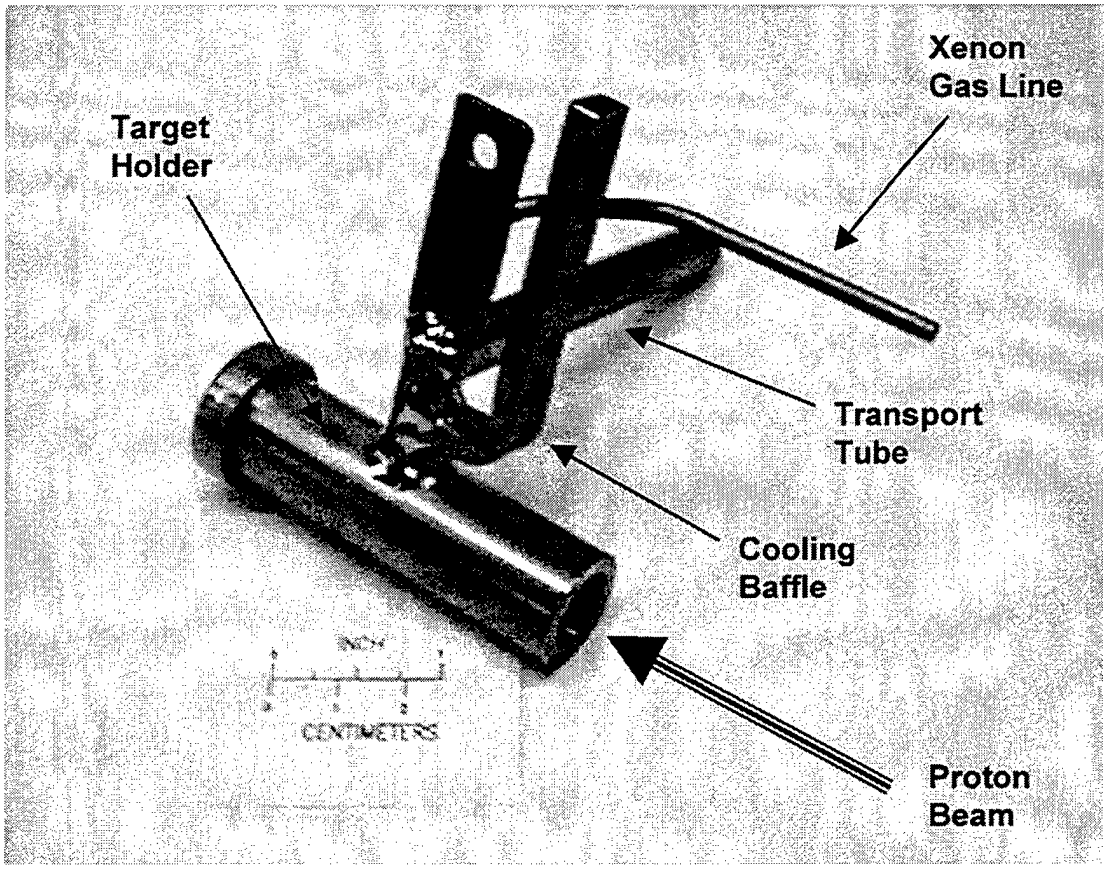

Figure 26. Photograph of Target Holder Assembly

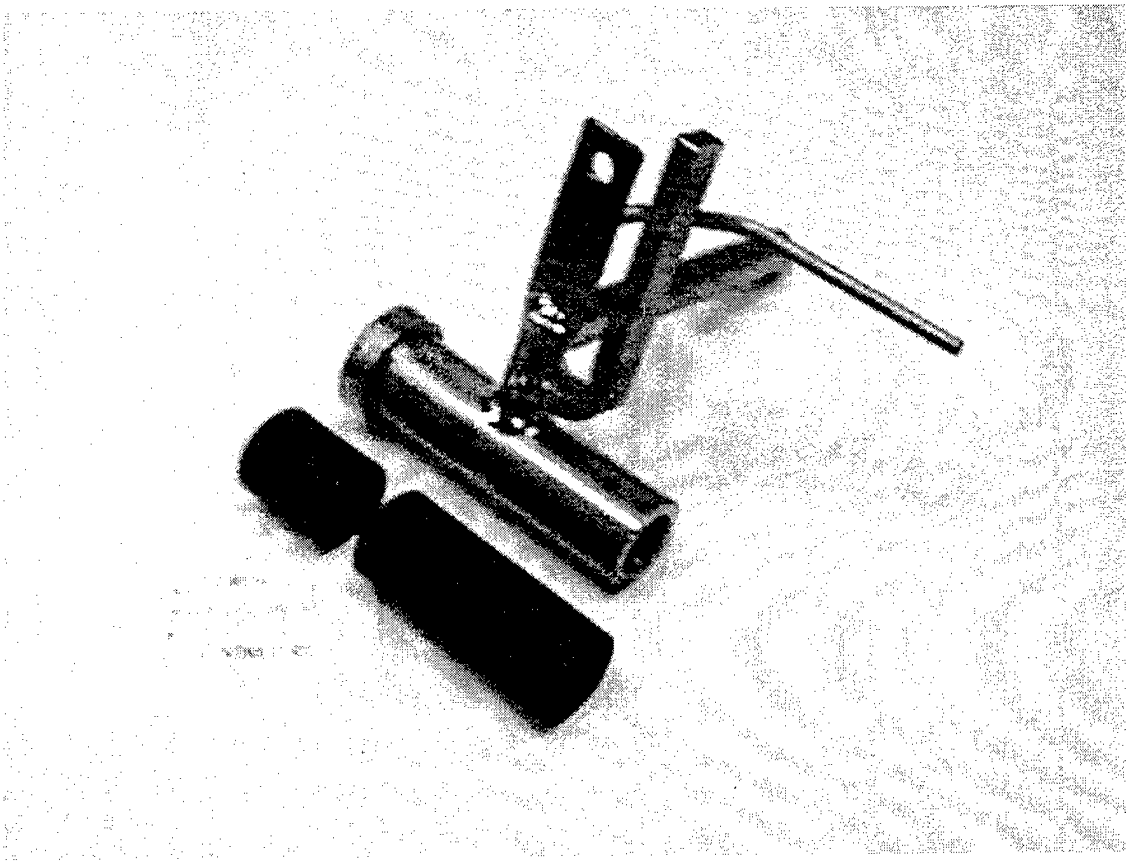

Figure 27. Photograph of Birdsnested Target Container Next to Target Holder Assembly. Carbon target container slips inside of the metal target holder shown behind it (appearances are deceiving).

F. CANDIDATE TARGET DESIGN DETAILS

We have already discussed many of the basic principles of the RIB production process and performed calculations needed to determine the target thickness of each of our four candidate target schemes. This section now addresses the design details and the motivations for each of the proposed target configurations.

1. The Planar Target

During actual RIB production, the TIS sits on a platform where the incident beam of protons enters the target 13° below the plane of the horizontal. This presents a unique opportunity to have liquid ^{70}Ge uniformly distributed on a horizontal W surface while simultaneously spreading the beam over a wide area. The 0.8 mm layer of Ge with the beam incidence angle of 77° is equivalent to a 3.5 mm thickness with a normal incidence beam. The first generation HRIBF target had a surface area of 0.4 cm^2 exposed to the vapor transport tube and the planar target 18.16 cm^2. Thus, the planar design realized a 48 times increase in open surface. Figures 28 and 29 are the drawing and photograph of this design.

A foreseen drawback is that the thickness of ^{70}Ge is less than 1.0 mm. With such a small layer, the material would tend to evaporate or be used in the production process well before the two-week life span that was hoped to be achieved [30]. To address this concern, a secondary reservoir of Ge was added and is shown in Figure 28. This would ensure that the material could be replenished in situ without having to shut down or exposing personnel to any potential unnecessary radiation hazards.

Total ion production rate is expected to be 9.5 x 10^{-4} atoms/ion for the planar target versus 9.2 x 10^{-4} for the first generation target. Since this target configuration has a much shorter mean diffusion path length $\bar{x}$ ~ 0.4 mm

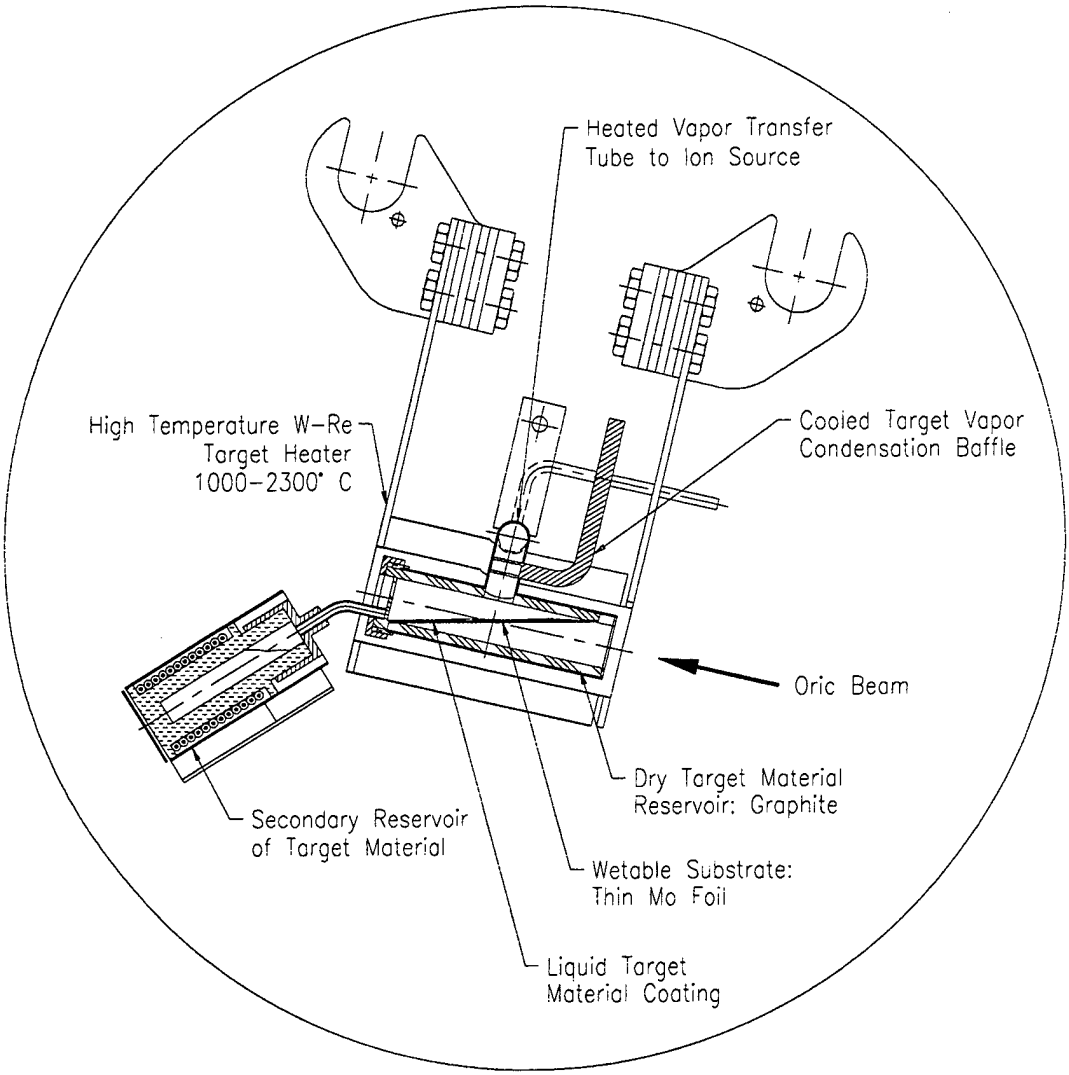

Figure 28. Recirculating Horizontal Liquid Metal Target System

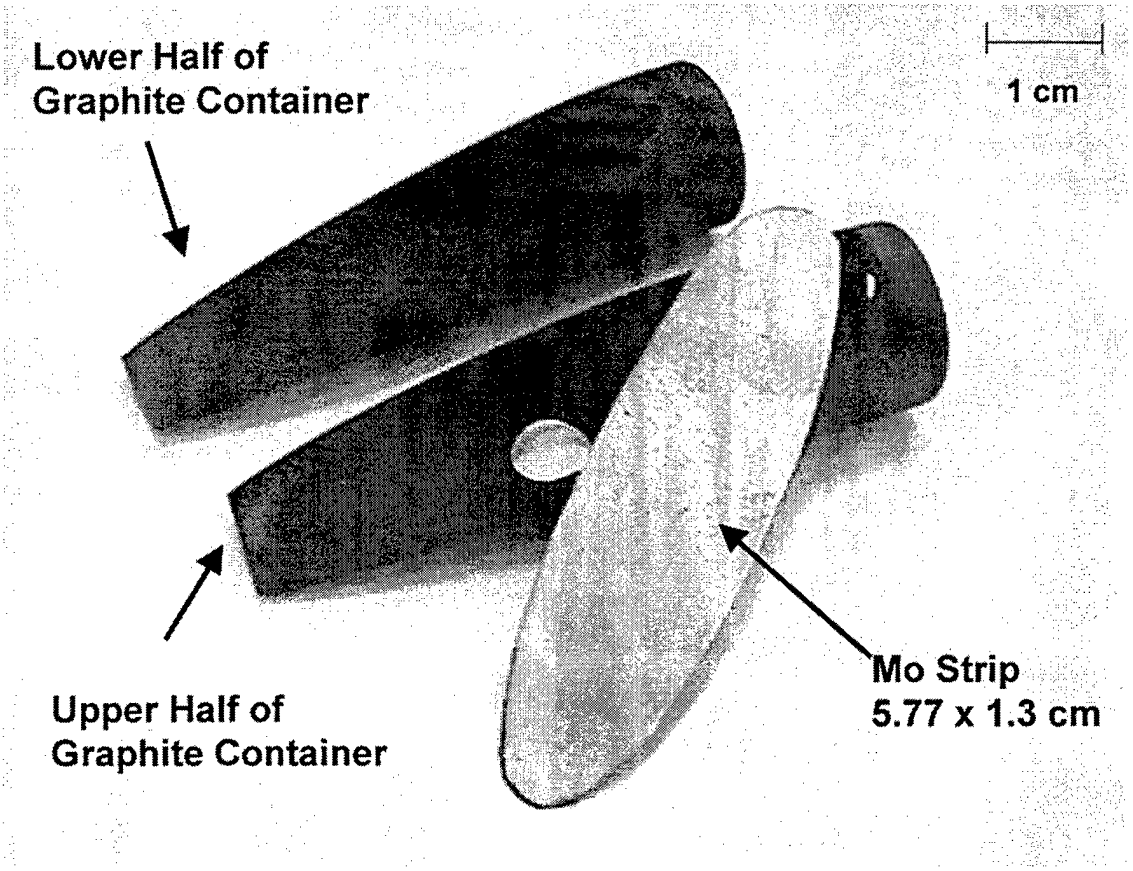

Figure 29. Photograph of Planar Strip with Graphite Container

versus $\bar{x}$ ~ 4.6 mm and increased yield of ^{69}As is expected from this configuration. Particularly when coupled with the re-circulating baffle discussed in section III.E.

2. The Birdsnested Target

This target configuration attempts to reduce the diffusion length still further by wetting a "birdsnested" Mo wire with molten Ge. This geometry also significantly increases the surface area of the target available to evaporate ^{69}As. A challenge was to ensure the produced ^{69}As had an avenue in which to transit to the ion source. The target was held at a porosity of 90%. This number was chosen somewhat arbitrarily and could be lower. Depending on the diameter of the Mo wire, ranging from 101 – 254 μm, the porosity varied from 89-90%. Once the specifications for a proposed target were determined, a SRIM calculation was run to ensure that the incident beam would exit with the right amount of energy, see section III.B. Exit beam energy was expected to be 17.5 MeV which worked out to be a 250 μm coating of Ge on a 254 μm diameter Mo wire substrate. Figures 27 and 30 are the photograph and drawing of the target configuration. The production rate is expected to be 6.73 x 10^{-4} atoms/ion. In this case, the mean diffusion path is much shorter ($\bar{x}$ ~ 0.25 mm) than the HRIBF first generation target path of $\bar{x}$ ~ 4.6 mm. This could correspond to an even greater increase of ^{69}As than the planar target.

3. The Fibrous Target

Two different forms of SiC were considered as a wetting substrate for Ge. The first is a commercially available weave composed of 15 μm SiC fibers bundles. A strip 25 cm x 1 cm of the weave material packed into the target container would have a surface area of about 375 cm^2. Calculations done earlier in the chapter require ~ 10 μm coating thickness of Ge. This target uses the

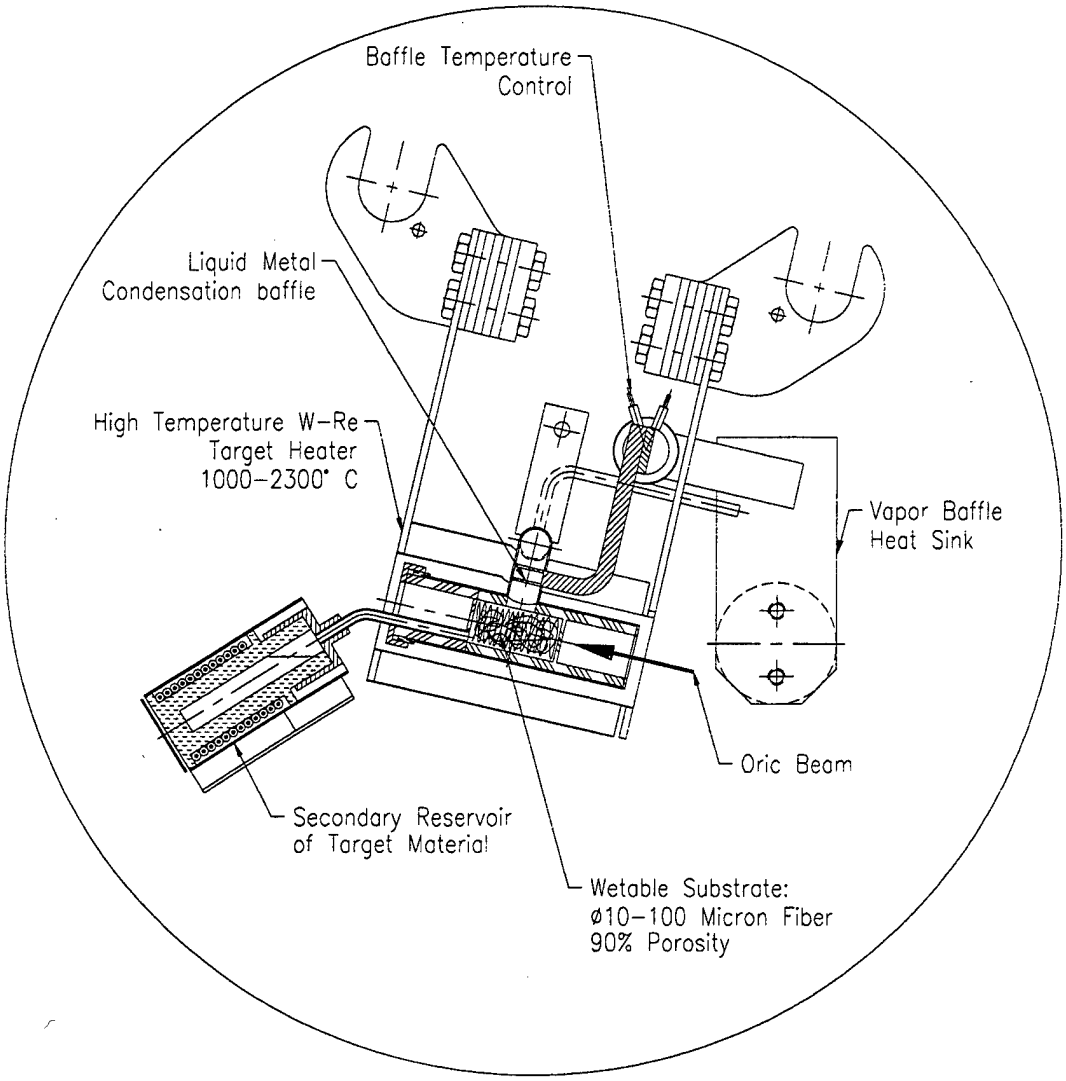

Figure 30. Very High Porosity Liquid Metal Target System

same target holder as the birdsnested target depicted in Figure 27. RADBEAM2 calculated the production rate to be 6.9 x 10^{-4} atoms/ion. Here the mean diffusion path was reduced from 4.6 mm in the HRIBF first generation target to ~0.005 mm.

When this target was tested in an ion source, it was found that the Ge did not wet the SiC fibers, but instead formed a pool at the base of the target holder. It is believed that a non-uniform temperature gradient was present during the wetting experiment, see Table 2 experiment 20. The Ge appeared to wet the SiC when in fact it may have been transported by sublimation or surface diffusion driven by this temperature gradient. This target configuration with SiC fibers is not deemed viable.

4. The Foam Target

The second form of SiC readily available is carbon foam chemical vapor deposited (CVD) coating of 10-15 μm SiC. Reticulated vitreous carbon (RVC) was used with a nominal 97% porosity and cross-links typically 100 μm in diameter. The porosity of the material when coated by Ge is calculated to be 92%. This target uses the same target holder as the birdsnested target depicted in Figure 27. RADBEAM2 calculated the production to be 8.4 x 10^{-4} atoms/ion. Here, the mean diffusion path should also be reduced from the 4.6 mm of the HRIBF first generation target to ~0.02 mm.

Table 4 is a summary of the four target designs and important design characteristic parameters.

Target	Surface Area (cm^2)	Coating Thickness	Substrate Dimensions			Exit Beam Energy (MeV)
			Diameter	*Width*	*Length*	
1st Generation	0.414	-	-	-	-	0
Planar	18.16	0.8 mm	2 cm (minor axis) 11.56 cm (major axis)	50.8 μm	-	15.05
Birdsnested	19.36	250 μm	250 μm	-	81.75 cm	17.50
Foam	86.86	41 μm	100 μm (Whiskers) 1.3 cm (Foam)	-	2.5 cm	19.20
Fibrous	375	9.6 μm	15 μm	1 cm	25 cm	14.42

Table 4. Target Design Characteristics Parameters.

IV. TARGET/ION SOURCE HEATING TESTS

Heating tests have so far been conducted on the birdsnested and SiC fibrous target configurations at UNISOR (University Isotope Separator at Oak Ridge) [31]. At the time of this writing, ^{69}As production tests have not yet been performed since the driver beam was not available. The tests did however provide a realistic test of the target system used in conjunction with an ion source as the target temperature was varied to determine if the structure was viable.

1. Experimental Equipment and Location

UNISOR, a facility located at HRIBF, can test prototype targets for durability and projected ion production. The experimental configuration of the system is similar to that used for high intensity RIB production; however, nanoampere test beams are used instead of microampere production beams used during normal operations. During December 1998, heating tests were conducted on the birdsnested target and in April 1999, heating tests were conducted on the SiC fibrous weave target. Data was recorded in UNISOR Log Book Number 5. Some information was also automatically recorded in Microsoft Excel files in the dedicated UNISOR computer. The prototype targets were heated with the coaxial target heaters shown in earlier figures. The target temperature was slowly raised to 1250 – 1450°C and Xe efficiency was continually checked.

Xe efficiency is a key indicator of ion source performance. Xe is introduced into the system at a fixed rate and the Xe ion current is measured. As the extracted Xe current changes, so does the ionization efficiency. The temperature where the Xe efficiency has dropped by a factor of three is generally very close to the maximum operating temperature of the new target. The configuration of the target in the test configuration is the same as online that is represented in Figure 30.

2. Results of Target Heating Tests

a. The Birdsnested Target

The initial test of the 250-μm Mo wire birdsnested target looked very promising. The target was first heated in the ion source with Ge in the liquid phase for about 20 hours (hour 28 to hour 48). Figure 31 shows the condition of a portion of the birdsnest after being removed from the target container. A uniform coating of Ge and very little target deterioration was noted. A second, longer test was run to estimate the lifetime of the target. It was during this test that the birdsnested target was at operational temperature for 80 hours. When the target material was removed from the graphite holder, it was discovered that the substrate had collapsed. Figure 32 shows the heating curves for the two tests conducted on this configuration.

About 3.4% Ge was lost in its 24 hours period, i.e. about 0.14% an hour. While maintaining structural integrity, the target should last for approximately 714 hours or 30 days before Ge would be entirely depleted; however, the second test suggests that the long-term stability of this prototype target is not satisfactory.

b. Fibrous SiC Target

The test of the SiC fibrous weave suggests that Ge does not wet SiC fibers. The target was gradually heated over a period of 52 hours with Ge being in the liquid phase for 31 hours (hour 20 to hour 51). Figure 33 shows the heating curve for the test. Post experiment examination of the target showed the SiC fibers to be flexible and the Ge had formed into a single ball. Loss of Ge was consistent with IV.2.a above. This test suggests that SiC fibers for this prototype design are not satisfactory.

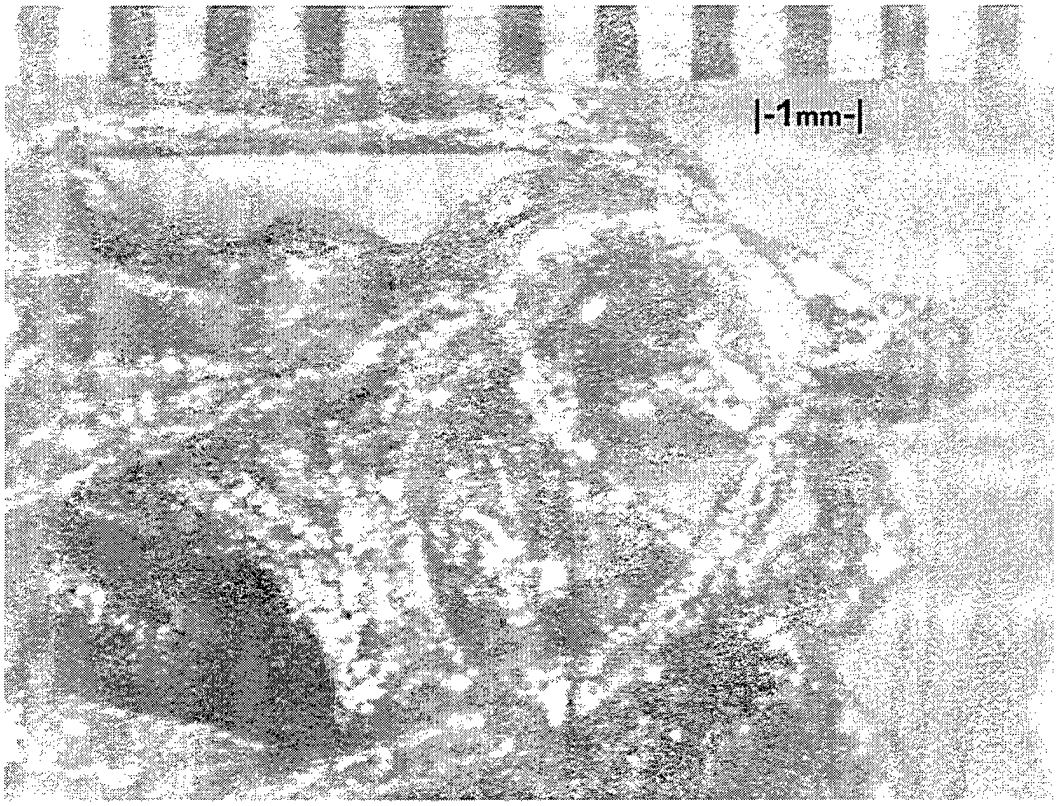

Figure 31. Photograph of Portion of Birdsnested Target after First UNISOR Test. 250-micron diameter Mo wire uniformly coated by ^{70}Ge after 20 hours at operational temperature.

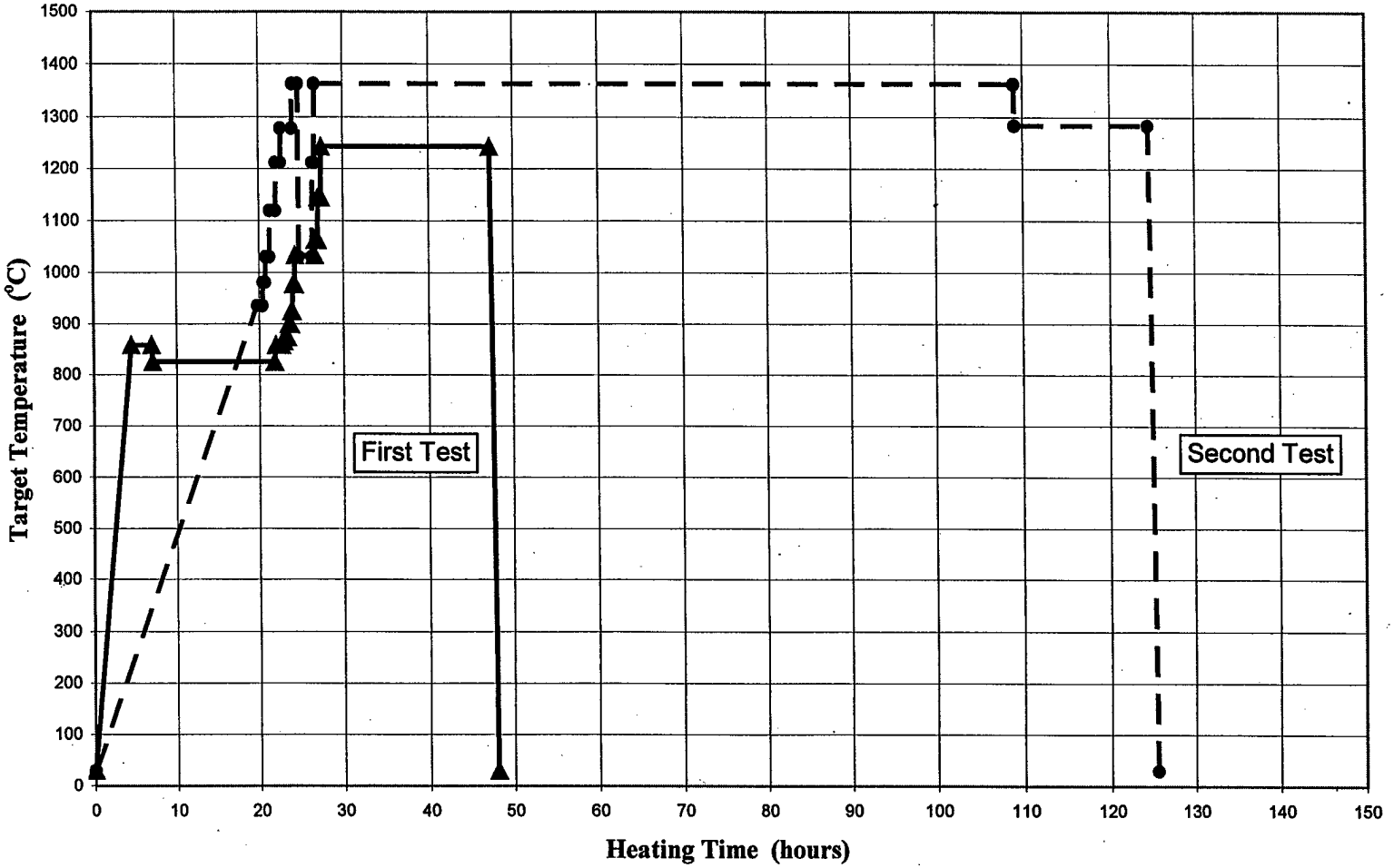

Figure 32. Heating Curve of Tests Conducted on Birdsnested Target at UNISOR.

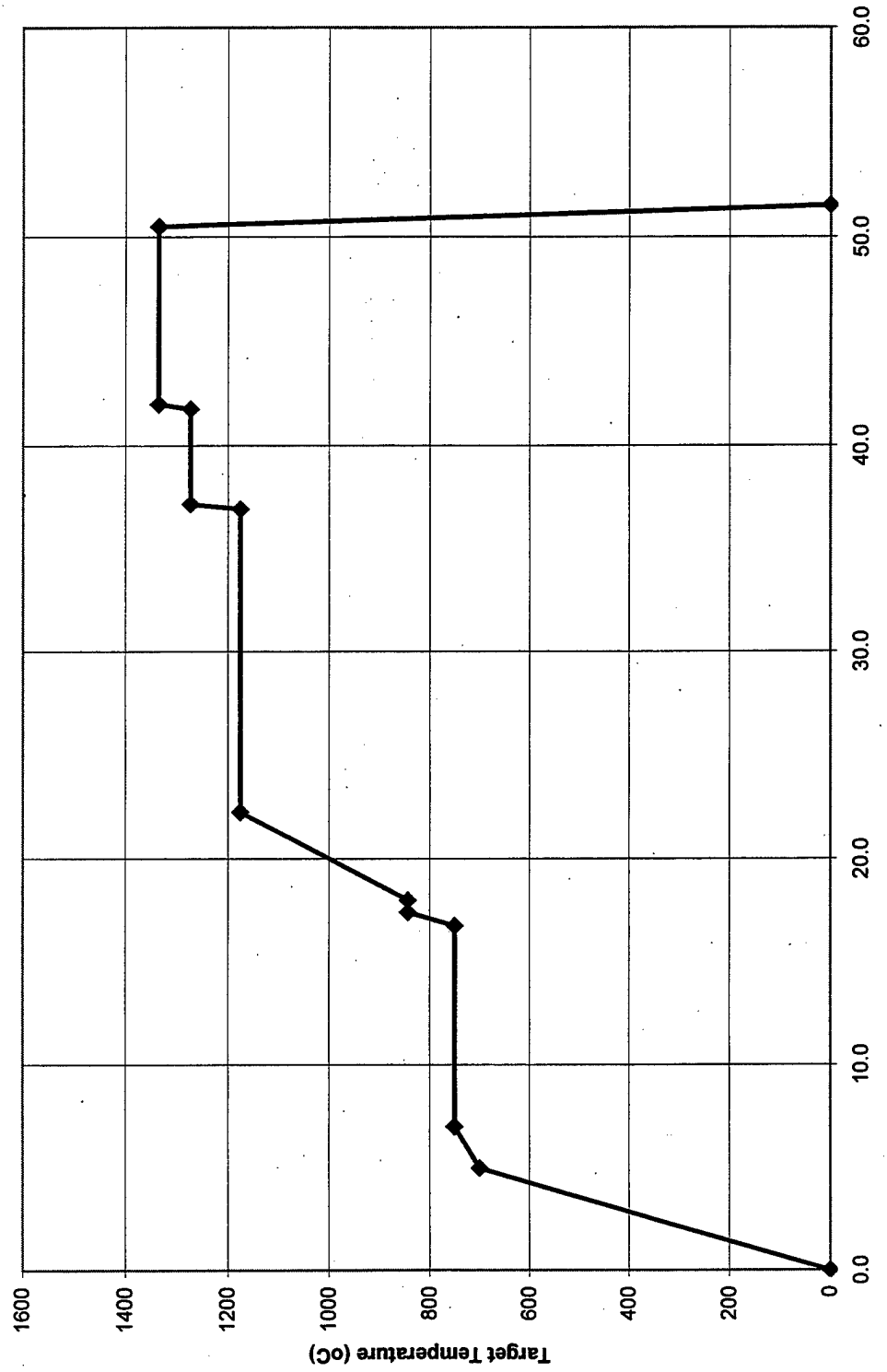

Figure 33. Heating Curve of Tests Conducted on SiC Fibrous Target at UNISOR.

V. CONCLUSION

This thesis work has been an initial investigation into the possibility of using open, highly pervious liquid targets as an alternative to traditional contiguous, pool-type targets for RIB generation. The candidate target systems developed here utilize wetting phenomenon to suspend very thin layers of liquid target material onto various substrates. Currently, RIBs of ^{69}As produced from liquid ^{70}Ge are desired at HRIBF for fundamental nuclear physics research. Toward this end, we have designed four candidate target systems which effectively reduce the mean diffusion path from several mm in the first generation Ge target used at the HRIBF to ~ 0.4 – 0.01 mm in the new target designs.

In order to locate a suitable wetting substrate material for Ge, several experiments were performed in a bell jar, Mo, W, and SiC were intially found to have favorable wetting properties when heated with Ge. A second experiment in which SiC and Ge were heated uniformly in a reservoir showed that virtually no wetting took place, despite previous reports found in literature to the contrary. The apparent wetting observed in the experiment #19 may have been caused by sublimation-condensation or surface diffusion caused by a temperature gradient present during the experiment.

Once suitable substrate materials had been selected, highly pervious target configurations needed to be envisioned and calculations performed to ensure a 42 MeV proton beam would exit the target with ~ 15 MeV. This exit energy was chosen since the cross section for ^{70}Ge (p, 2n) ^{69}As reaction becomes negligible below this value, while the deposited beam power density increases significantly. The maximum proton beam energy that can be provided by ORIC is currently 42 MeV.

The first prototype target configuration developed was a planar target which a thin W window was uniformly coated with a layer of Ge held in a graphite container. This window was inclined 13° with respect to the beam axis, shown in Figure 24, to (i) reduce the mean diffusion path to ~400 μm and (ii) increase the

effective radiating surface area of the target for heat removal. This target has been constructed and currently awaits testing.

The second prototype target configuration developed was a birdsnested ~250 μm Mo wire uniformly coated by ~250 μm of Ge held in a graphite container. The effective mean diffusion path of this configuration was ~125 μm, much lower than the first generation HRIBF design. The porosity was maintained at 90% to allow product atoms a release path from the birdsnest. This target system was tested and shown to survive for a period of at least 20 hours at a uniform temperature of ~1250°C. A second test at ~1360°C showed the structural integrity of the Mo birdsnest was compromised in <100 hours, which indicates that this configuration is not suitable for long-term generation. This matrix, however, is scheduled for low intensity tests at UNISOR to verify that ^{69}As yield can be improved through this approach.

The third prototype target configuration developed was based on a fibrous weave of 15 μm bundles of SiC rolled into to cylindrical volume. Once coated with 9 μm of ^{70}Ge this target has a porosity of 85% allowing a release path from the woven material. In this case, the mean diffusion path in this configuration would be ~ 8 μm, which is again much lower than the first generation HRIBF design (x ~ mm). Unfortunately, when tested in a RIB-TIS, this configuration anomalously exhibited no wetting by Ge and is therefore not deemed to be a viable RIB target.

The fourth prototype target configuration developed was also based on SiC, this time in the form of carbon foam CVD coated with 10-15 μm SiC. RVC was used with a nominal 97% porosity and cross-links typically 100 μm in diameter. Once coated with ~40 μm of Ge, this target would also be characterized by a high porosity and short mean diffusion path ~20 μm. Because of the conflicting results from the Ge / SiC wetting experiments, development of this target has been suspended until the wetting properties of SiC can be clarified.

Each of the above candidate targets were designed to fit into a universal Ta target holder and re-circulating baffle. The design of this system was also undertaken as part of this thesis project. By introducing a cooled baffle between the target and ion source, the loss of target can be minimized by condensation and return of the liquid to the target container. The temperature of this baffle is controlled by a secondary heater affixed to the baffles heat sink. This structure has been tested without the secondary heater and has been shown to perform adequately.

Although much of the target systems designed here have not yet been tested on-line, this work has provided the essential apparatus needed for definitively ascertaining the value of implementing highly pervious liquid targets over the traditional pool-type configurations. If the on-line tests are successful and substantial yield increases can be achieved for ^{69}As from ^{70}Ge, other RIBs produced from highly pervious liquid targets will be developed. For example, RIBs of short-lived ^{58}Cu are in considerable demand. A liquid ^{58}Ni target would be ideal for this species. The literature suggests TiC can be thoroughly wet by Ni. Thus a Ni / TiC target could developed for ^{58}Cu by using the same experimental and target design procedures outlined in this thesis.

LIST OF REFERENCES

1. L. Valyi, *Atom and Ions Sources*, John Wiley & Sons, Inc., 1977.
2. H.L Ravn, *Radioactive Nuclear Beam facilities based on ISOL-Postaccelerator Schemes*, CERN-PPE/91-173, 10 April 1991.
3. H.L Ravn, P. Bricault, G. Ciavola, P. Drumm, B. Fogelberg, E. Hagebø, M. Huyse, R. Kirchner, W. Mittig, A. Mueller, H Nifenecker, and E. Roeckl., *Comparison of Radioactive Ion-Beam Intensities Produced by Means of Thick Targets Bombarded with Neutrons, Protons, and Heavy Ions*, CERN-PPE/93-102, 6 February1993.
4. B.M. Sherill, Nuclear Physics A 621(1997) C203-C210.
5. J.R. Parrington, H.D Knox, S.L. Breneman, E.M. Baum, and F. Feiner, *Nulclides and Isotopes*, 15th ed., 1996.
6. J.D. Garrett, *The Latest from the New Holifield Radioactive Ion Beam Facility at Oak Ridge National Laboratory*, Nuclear Physics A616 (1997) 3c-10c.
7. R.L. Auble, "The Production and Acceleration of Radioactive Ion Beams at the HRIBF", *Proceedings of the Fifteenth International Conference on the Application of Accelerators to Research and Industry*, Denton, TX, AIP Press, Woodbury, New York, 4-6 Nov 1998.
8. R. F. Welton, G.D. Alton, B. Cui, and S.N. Murray, *Experimental Methods in Radioactive Ion-Beam Target/Ion Source Development and Characterization*, pp. 2892-2897, Review of Scientific Instruments, Vol 68 N. 8, August 1998.
9. H.L Ravn, "Sources for Production of Radioactive Ion-Beams", [http:///www.cern.cg/accelconf/p95/ARTICLES/MPE/MPE02.PDF], 4 March 1994.

10. E. Hagebø, *Proc. Int. Conf. On Electromagnetic Isotope Seperators and the Techniques of Their Applications*, pp. 146, Marburg, 1970, eds H. Wagner and W. Walcher BMBW-FB K 70-28, 1970.
11. H. Andreasen, R. Eder, H. Grawe, H. Haas, E. Hagebø, P. Hoff, H.L. Ravn, K. Steffensen, and S. Sundell, *Mixtures of Molten Metals and Graphite as Targets for On-Line Mass Separators*, European Organization for Nuclear Research, 14 January 1991.
12. J.F. Liang, *Private Communication*, September 1998.
13. H.K. Carter, J. Kormicki, D.W. Stracner, J.B. Breitenbach, J.C. Blackmoon, M.S. Smith, and D.W. Bardayan, *First On-Line Results for As and F Beams from HRIBF Target/Ion Sources*, Nuclear Instruments and Methods in Physics Research B 126, 1997.
14. Dr. R. Welton, *Private Communication*, September 1998.
15. M. Santella, *Private Communication*, December 1998.
16. T. Iseki, K. Yamashita, and H. Suzuki, *Joining of Self-Bonded SiC by Ge Metal*, pp. 1-8, Proceedings British Ceramics Society, 31, 1981.
17. *NRC 3117 Bell Jar Vacuum System Instruction Manual*, Serial Number 24937-001, Norton Co., October 1969.
18. *8627 Series Optical Pyrometers Instruction Manual*, 177720 Rev E, Leeds & Northrup.
19. K.J. Ross, *High Temperature Metal Atom Beam Sources*, Rev. Sci. Instrum. 66(9), September 1995.
20. T. Iida, Roderick, and I. L. Gutherie, *The Physical Properties of Liquid Metals,* Clarendon Press, 1988.
21. M. Fujioka and Y. Arai, *Diffusion of Radioisotopes from Solids in the Form of Foils, Fibers and Particles*, pp. 409, Nuclear Instruments and Methods 186, 1981.

22. H.L. Ravn, *Experiments with Intense Sceondary Beams of Radioactive Ions*, pp. 201-259, Physics Reports (Review Section of Physics Letters) 54 No. 3, 1979.
23. P.D. Townsend, J.C. Kelley, and N.E.W. Hartley, *Ion Implantation, Sputtering and their Applications*, Academic Press Inc., 1976.
24. J. F. Ziegler, "The Stopping Range of Ions in Matter", [http://www.research.ibm.com/ionbeams/SRIM], September 1998.
25. K. S. Krane, *Introductory Nuclear Physics*, John Wiley & Sons, Inc., 1988.
26. J. Gomez Del Campo, *Private Communication*, September 1998.
27. J. Gomez Del Campo, *Private Communication*, November 1998.
28. Dr. R. F. Welton, *Private Communication*, August 1998.
29. A. Roine, *Outokumpu HSC Chemistry for Windows, Chemical Reaction and Equilibrium Software with extensive Thermochemical Database*, Version 2.0, Outokumpu Research Oy, 31 May 1994
30. D. Stracener, *Private Communication*, December 1998.
31. H.K. Carter, P.F. Mantica, J. Kormicki, C. A. Reed, A.H. Poland, W.L. Croft, and E.F. Zganjar, *UNISOR Separator Upgrade*, Physics Division Progress Report ORNL-6842, Martin Marietta Energy Systems, Inc, Oak Ridge National Laboratory, 30 September 1994.

INITIAL DISTRIBUTION LIST

1. Defense Technical Information Center 2
   8725 John J. Kingman Rd., STE 0944
   Ft. Belvoir, Virginia 22060-6218

2. Dudley Knox Library 2
   Naval Postgraduate School
   411 Dyer Rd.
   Monterey, California 93943-5101

3. ORNL Physics Division Library 1
   Oak Ridge National Laboratory
   Building 6000, Mailstop 6371
   PO Box 2008
   Oak Ridge, Tennessee 37831-6371

4. University Isotope Separator at Oak Ridge (UNISOR) 1
   Oak Ridge National Laboratory
   Building 6000, Mailstop 6368
   PO Box 2008
   Oak Ridge, Tennessee 37831-6368

5. Dr. Robert F. Welton 5
   Oak Ridge National Laboratory
   Building 6000, Mailstop 6368
   PO Box 2008
   Oak Ridge, Tennessee 37831-6368

6. Breckenridge S. Morgan 5
   824 Amy Street
   Seymour, Tennessee 37865

7. Dr. William B. Maier II 5
   Chairman, Physics Department
   Naval Postgraduate School
   411 Dyer Rd.
   Monterey, California 93943-5101

8. Engineering & Technology Curricular Office, Code 34 1
   Naval Postgraduate School
   411 Dyer Rd.
   Monterey, California 93943-5101